Mononuclear and Binuclear Molybdenum(V) Complexes of the Ligand *N,N′*-Dimethyl-*N,N′*-bis(2-mercaptophenyl)ethylenediamine: Geometric Isomers

Keith R. Barnard,[†] Michael Bruck,[‡] Susan Huber,[‡] Carina Grittini,[‡] John H. Enemark,[‡] Robert W. Gable,[†] and Anthony G. Wedd*[,†]

School of Chemistry, University of Melbourne, Parkville, Victoria 3052, Australia, and Department of Chemistry, University of Arizona, Tucson, Arizona 85721

Received July 18, 1996[⊗]

The syntheses of mononuclear complexes *cis*-$Mo^{V}OXL$ (X = Cl, Br, OMe, OEt, OPh, SPh, NCS, $OSiMe_3$) and two binuclear complexes $Mo^{V}_2O_3L_2$ of the title ligand LH_2 are reported. Two forms of MoOClL, with *cis* oxo and chloro ligands, were crystallized, one in space group $P2_1/n$, with $a = 10.440(2)$ Å, $b = 14.260(2)$ Å, $c = 12.041(2)$ Å, $\beta = 102.76(2)°$, $V = 1748(1)$ Å^3, and $Z = 4$, and the other in $P2_1/c$, with $a = 13.564(4)$ Å, $b = 7.172(2)$ Å, $c = 18.242(6)$ Å, $\beta = 95.19(1)°$, $V = 1767(2)$ Å^3, and $Z = 4$. MoO($OSiMe_3$)L crystallizes in space group $P2_1/c$, with $a = 15.923(3)$ Å, $b = 11.141(2)$ Å, $c = 14.186(2)$ Å, $\beta = 112.64(2)°$, $V = 2323(1)$ Å^3, and $Z = 4$, while MoO(NCS)L crystallizes in $Pna2_1$, with $a = 22.471(2)$ Å, $b = 12.136(2)$ Å, $c = 7.138(1)$ Å, $V = 1947(1)$ Å^3, and $Z = 4$. The four structures reveal two possible conformations for ligand L: one with *trans* S atoms (*cis,trans*-MoOClL and -MoO($OSiMe_3$)L) and one with *cis* S atoms (*cis,cis*-MoOClL and -MoO(NCS)L). The *cis,cis* isomers are converted to the *cis,trans* forms under reflux in MeCN at 80 °C. Only the *cis,trans* forms could be isolated for bulkier ligands X (OPh, SPh, $OSiMe_3$). A short $H_3C\cdots X$ interaction is present in the *cis,cis* forms: $C\cdots Cl = 3.07$ Å and $C\cdots N = 2.93$ Å, for X = Cl and NCS, respectively. Infrared and electronic spectral data provide unambiguous identification of the stereochemistry of ligand L in mononuclear complexes MoOXL. Effective removal of ligand X = OR from *cis,cis*-MoO(OR)L (R = Me, Et) led to two binuclear complexes $(Mo^{V}OL)_2(\mu\text{-O})$ of C_i and C_1 point symmetries. C_i-$(MoOL)_2(\mu\text{-O})\cdot$thf crystallizes in space group $P2_1/c$, with $a = 8.5650(5)$ Å, $b = 15.1862(9)$ Å, $c = 16.8038(9)$ Å, $\beta = 100.183(1)°$, $V = 2157.1(8)$ Å^3, and $Z = 2$, while C_1-$(MoOL)_2(\mu\text{-O})\cdot CH_2Cl_2$ crystallizes in space group $P2_1/c$, with $a = 12.5250(5)$ Å, $b = 24.673(1)$ Å, $c = 12.7253(6)$ Å, $\beta = 108.070(4)°$, $V = 3738.6(3)$ Å^3, and $Z = 4$. C_i-$(MoOL)_2(\mu\text{-O})\cdot$thf features two *cis,trans*-$Mo^{V}OXL$ centers with X = μ-O, while C_1-$(MoOL)_2(\mu\text{-O})\cdot CH_2Cl_2$ contains a *cis,trans* and a *cis,cis* center. In the latter, the Mo−O−Mo link is asymmetric, allowing relief of steric crowding on the *cis,cis* side of the molecule.

Introduction[1]

The pterin-containing molybdenum enzymes catalyze exchange of an oxygen atom between substrate X and water.[2−6] In formal terms, eqs 1−3 summarize the redox chemistry.

$$X + Mo^{VI}O = XO + Mo^{IV} \quad (1)$$

$$Mo^{IV} + H_2O = Mo^{VI}O + 2H^+ + 2e^- \quad (2)$$

$$\text{net:} \quad X + H_2O = XO + 2H^+ + 2e^- \quad (3)$$

Equation 1 seems to be a concerted $2e^-$ event (oxygen atom transfer), while the regeneration of the active site (eq 2) appears to be achieved in two $1e^-$ steps via Mo(V) (coupled electron−proton transfer).[4−6] A combination of X-ray absorption and EPR spectroscopies for various enzymes and for analog species augmented by equilibrium electrochemical techniques has defined the partial coordination spheres at the Mo(VI), Mo(V), and Mo(IV) levels. Figure 1 documents those for two of the more intensively studied oxidase enzymes, sulfite oxidase (SO) and xanthine oxidase (XnO). At least one oxo ligand is proposed for each redox level, and two of the thiolate ligands are supplied by an ene-1,2-dithiolate function of the molybdopterin cofactor.[7] A crystal structure for an oxidized form of aldehyde oxidoreductase from *Desulfovibrio gigas* reveals a $[Mo^{VI}O_2(OH)]$ fragment bound by an ene-1,2-dithiolate in a five-coordinate site.[8]

A synthetic system based upon *cis,trans*-$Mo^{VI}O_2L$ (LH_2: structure **I**) has allowed the *cis* isomers of $[Mo^{V}O_2L]^-$, $Mo^{V}O(OH)L$, $[Mo^{V}OSL]^-$, and $Mo^{V}O(SH)L$ to be generated

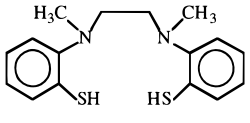

LH_2

I

* Corresponding author. E-mail: t.wedd@chemistry.unimelb.edu.au.
† University of Melbourne.
‡ University of Arizona.
⊗ Abstract published in *Advance ACS Abstracts,* January 1, 1997.

(1) Abbreviations: EPR, electron paramagnetic resonance; SO, sulfite oxidase; XnO, xanthine oxidase; LH_2, *N,N′*-dimethyl-*N,N′*-bis(2-mercaptophenyl)ethylenediamine; L*H2, *N,N′*-dimethyl-*N,N′*-bis(2-mercaptoethyl)ethylenediamine; $qtlH_2$, 8-mercaptoquinoline; thf, tetrahydrofuran.

(2) Bray, R. C. *Q. Rev. Biophys.* **1988**, *21*, 299.
(3) Holm, R. H. *Coord. Chem. Rev.* **1990**, *100*, 183.
(4) Young, C. G.; Wedd, A. G. In *Molybdenum Enzymes, Cofactors and Model Systems*; Stiefel, E. I., Coucouvanis, D., Newton, W. E., Eds.; ACS Symposium Series 535; American Chemical Society: Washington, DC, 1993; p 70.
(5) Enemark, J. H.; Young, C. G. *Adv. Inorg. Chem.***1993**, *40*,1.
(6) Young, C. G.; Wedd, A. G. In *Encyclopedia of Inorganic Chemistry*; King, R. B., Ed.; Wiley: New York, 1994; p 2330.
(7) (a) Rajagopalan, K. V. *Adv. Enzymol. Relat. Areas Mol. Biol.* **1991**, *64*, 215. (b) Rajagopalan, K. V.; Johnson, J. L. *J. Biol. Chem.* **1992**, *267*, 10199.
(8) Ramao, M. J.; Archer, M.; Moura, I.; Moura, J. J. G.; LeGall, J.; Engh, R.; Schneider, M.; Hof, P.; Huber, R. *Science* **1995**, *270*, 1170.

S0020-1669(96)00848-8 CCC: $14.00

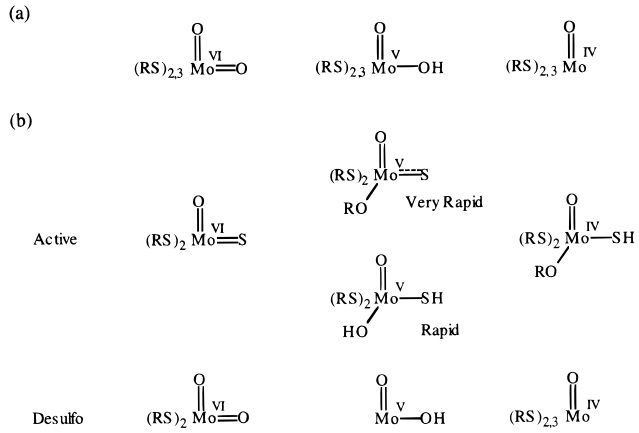

Figure 1. Partial coordination spheres for Mo(VI), Mo(V), and Mo(IV) forms of (a) sulfite oxidase and (b) xanthine oxidase.

in solution.[9−11] Detailed comparison of ^{1}H, ^{17}O, ^{33}S, and ^{95}Mo hyperfine couplings in EPR spectra of these species and those of SO and XnO[2,12] assisted definition of the Mo^{V} coordination spheres depicted in Figure 1. However, detailed structural information for the above complexes of ligand L is confined to *cis,trans*-$Mo^{VI}O_2L$ only.[9]

This paper reports the synthesis of 11 mononuclear *cis*-Mo^{V}-OXL compexes (X = Cl, Br, OMe, OEt, OPh, SPh, NCS, $OSiMe_3$) and two binuclear $(Mo^{V}OL)_2(\mu$-O) complexes. Structural characterization of four of the mononuclear and both binuclear species by X-ray crystallography reveals an interesting structural versatility associated with quadridentate ligand L. Two conformations are possible: one with *trans* S atoms (MoOClL, $MoO(OSiMe_3)L$, C_i-$(MoOL)_2(\mu$-O)) and one with *cis* S atoms (MoOClL, MoO(NCS)L). Both conformations are present in C_1-$(MoOL)_2(\mu$-O). The presence of a given conformation is signaled by differences in the spectroscopic and electrochemical properties of individual complexes.

Experimental Section

Materials. Syntheses of the molybdenum compounds were performed using standard Schlenk techniques under purified dinitrogen. Reagent grade solvents were dried and fractionally distilled under dinitrogen.[10] Microanalyses were performed by either the Analytische Laboratorien, Elbach, Germany, or Atlantic Microlabs Inc., Norcross, GA.

cis-$Mo^{VI}O_2(acac)_2$,[13] (pyH)[$Mo^{V}OBr_4$],[14] and $A_2[Mo^{V}OCl_5]$ (A = pyH,[14] NH_4[15]) were synthesized by literature methods. For LH_2,[9] refinement of two of the steps in the synthesis led to an increase in total yield from 18 to 30%. In the preparation of the intermediate *N*,*N*′-dimethyl-*N*,*N*′-bis(2-(benzylthio)phenyl)ethylenediamine, glyoxal:*N*-methyl-2-(benzylthio)aniline and $ZnCl_2$:*N*-methyl-2-(benzylthio)aniline ratios of 1:3 and 1:2.7, respectively, were employed along with a longer stirring time of 4 h. The final step was performed on a 5-fold scale using 20% more sodium metal and 33% less butanol. NaNCS, $NaOSiMe_3$, and PPh_3 were purchased from Aldrich. NaOMe and NaOEt were prepared by reaction of sodium metal with the appropriate alcohol, filtering, and removing excess solvent under vacuum to yield a white, free-flowing powder. NaOPh was prepared by the reaction of NaOH with phenol via a previously published method.[16] To prevent possible loss of the label, NaOPh (45 atom % ^{17}O) was prepared by reaction of sodium metal and labeled PhOH (CIL Laboratories) in rigorously dried tetrahydrofuran (thf). NaSPh was prepared similarly from NaOH and freshly distilled thiophenol.

***cis,trans*-$Mo^{VI}O_2L$.** This complex was synthesized as previously reported[9] and is further characterized here: ν(MoO) 921, 894 cm^{-1}; EI-MS *m/z* 432; ^{1}H NMR ($CDCl_3$) 7.31−7.38 (m, Ph, 4 protons), 7.12−7.18 (m, Ph, 4), 3.67 (s, CH_3, 6), 3.27 (d, 11.0 Hz, CH_2, 2), 2.89 ppm (d, 10.8 Hz, CH_2, 2); ^{13}C NMR ($CDCl_3$) 150.5, 139.4, 129.9, 128.3, 126.1, 122.4, 62.2, 51.8 ppm.

***cis,cis*-MoOClL.** This complex[9] can be synthesized from $(NH_4)_2$-$[MoOCl_5]$ or from $(pyH)_2[MoOCl_5]$. In the latter case, pyHCl is separated from the crude product by washing with MeOH. X-ray-quality crystals were grown in air by the slow diffusion of a CH_2Cl_2 solution into a layer of hexane; crystals were isolated after 22 h. Anal. Calcd for $C_{16}H_{18}ClMoN_2OS_2$: C, 42.7; H, 4.0; N, 6.2; Cl, 7.9. Found: C, 42.5; H, 4.2; N, 6.1; Cl, 8.0. EI-MS: *m/z* 451. *cis,cis*-[^{98}MoOClL] (97 atom % ^{98}Mo) was prepared from enriched $(pyH)_2$-$[^{98}MoOCl_5]$.[14]

***cis,trans*-MoOClL.** A stirred solution of *cis,cis*-MoOClL (0.15 g, 0.33 mmol) in MeCN (35 cm^3) was refluxed for 2 h. Solvent was removed under vacuum, the residue extracted with a minimum of CH_2Cl_2, and the extract applied to a silica gel column (mesh 70−230; 42 cm × 2.3 cm) in air. The first green band which appeared upon elution with CH_2Cl_2 (13 cm^3 min^{-1}) was collected. This was concentrated to 6 cm^3 and layered with hexane (7 cm^3) in air. Evaporation over 3 days yielded X-ray-quality crystals, which were washed with *n*-hexane and dried in vacuum (0.10 g, 67%). Anal. Calcd for $C_{16}H_{18}ClMoN_2OS_2$: C, 42.7; H, 4.0; N, 6.2; Cl, 7.9. Found: C, 42.7; H, 4.1; N, 6.3; Cl, 8.0. EI-MS: *m/z* 451.

***cis,cis*-MoO(NCS)L.** A solution of NaNCS (0.098 g, 1.2 mmol) in EtOH (4 cm^3) was added dropwise to a stirred solution of *cis,cis*-MoOClL (0.52 g, 1.2 mmol) in CH_2Cl_2 (40 cm^3). After 1.25 h, the solvent was removed under vacuum, the residue extracted with CH_2Cl_2 (24 cm^3), and the solution filtered through Celite. Hexane (10 cm^3) was added and the volume reduced to 16 cm^3. After 2.5 h of standing at −20 °C, the dark green crystals were filtered off, washed twice with hexane and dried under vacuum (0.39 g, 54%). Anal. Calcd for $C_{17}H_{18}$-MoN_3OS_3: C, 43.2; H, 3.8; N, 8.9; S, 20.4. Found: C, 43.1; H, 3.9; N, 8.8; S, 20.2. EI-MS: *m/z* 474. X-ray-quality crystals were grown by layering *n*-hexane (2 cm^3) over a solution of the compound (0.025 g) in CH_2Cl_2 (2 cm^3).

***cis,cis*-MoOBrL.** A solution of LH_2 (1.3 g, 4.2 mmol) in CH_2Cl_2 (14 cm^3) was added dropwise to a stirred solution of (pyH)[$MoOBr_4$] (2.2 g, 4.2 mmol) in MeOH (18 cm^3). After 0.75 h, the solvent was removed under vacuum, the product was stirred with EtOH (24 cm^3), the mixture was filtered to remove pyHCl, and the solid was washed twice with EtOH and dried in vacuum (1.8 g, 85%). Anal. Calcd for $C_{16}H_{18}BrMoN_2OS_2$: C, 38.9; H, 3.7; N, 5.7; Br, 16.2. Found: C, 38.7; H, 3.8; N, 5.6; Br, 16.4. EI-MS: *m/z* 495.

***cis,cis*-MoO(OMe)L.** A solution of NaOMe (0.77 g, 1.4 mmol) in MeOH (7.3 cm^3) was added dropwise to a stirred solution of *cis,cis*-MoOClL (0.6 g, 1.3 mmol) in CH_2Cl_2 (35 cm^3). After 0.75 h, the solvent was removed under vacuum, the residue extracted with CH_2Cl_2 (38 cm^3), the solution filtered through Celite, and the volume reduced to 18 cm^3. $Pr^{i}OH$ (10 cm^3) was added and a further 10 cm^3 of solvent removed. After 12 h of standing at −20 °C, the deep purple-red microcrystals were filtered off, washed three times with Et_2O, and dried under vacuum (0.24 g, 41%). Anal. Calcd for $C_{17}H_{21}MoN_2O_2S_2$: C, 45.8; H, 4.8; N, 6.3; O, 7.2. Found: C, 45.6; H, 4.7; N, 6.2; O, 7.4. EI-MS: *m/z* 447.

***cis,cis*-MoO(OEt)L.** This complex was prepared similarly as an amorphous purple-red solid (0.16 g, 41%). EI-MS: *m/z* 461.

***cis,trans*-MoO(NCS)L.** A stirring solution of *cis,cis*-[MoO(NCS)L] (0.077 g, 0.16 mmol) in MeCN (14 cm^3) was refluxed for 4 h. Solvent was removed under vacuum, the residue extracted with CH_2Cl_2 (6 cm^3), and the extract applied to a silica gel column (mesh 70−230, 20 cm × 2.3 cm diameter) in air. The first (green) band that appeared upon

(9) Dowerah, D.; Spence, J. T.; Singh, R.; Wedd, A. G.; Wilson, G. L.; Farchione, F.; Enemark, J. H.; Kristofzski, J.; Bruck, M. J. *J. Am. Chem. Soc.* **1987**, *109*, 5655.
(10) Wilson, G. L.; Greenwood, R. J.; Pilbrow, J. R.; Spence, J. T.; Wedd, A. G. *J. Am. Chem. Soc.* **1991**, *113*, 6803.
(11) Greenwood, R. J.; Wilson, G. J.; Pilbrow, J. R.; Wedd, A. G. *J. Am. Chem. Soc.* **1993**, *115*, 5385.
(12) Bray, R. C. *Adv. Enzymol. Relat. Areas Mol. Biol.* **1980**, *51*, 107.
(13) Chen, G. J.-J.; McDonald, J. W.; Newton, W. E. *Inorg. Chem.* **1976**, *15*, 2612.
(14) Hanson, G. R.; Brunette, A. A.; McDonell, A. C.; Murray, K. S.; Wedd, A. G. *J. Am. Chem. Soc.* **1981**, *103*, 1953.
(15) Saha, H. K.; Banerjee, A. K., *Inorg. Synth.* **1984**, *15*, 100.
(16) Kornblum, N.; Lurie, A. P. *J. Am. Chem. Soc.* **1959**, *81*, 2705.

elution with CH_2Cl_2 (12 cm^3 min^{-1}) was collected, concentrated (4 cm^3), and layered with *n*-hexane (4 cm^3). Evaporation over 3 days yielded dark green plates, which were washed with *n*-hexane and dried under vacuum (0.060 g, 0.13 mmol, 78%). Anal. Calcd for $C_{17}H_{18}MoN_3OS_3$: C, 43.2; H, 3.8; N, 8.9. Calcd for $C_{17}H_{18}MoN_3OS_3 \cdot {}^1/_2CH_2Cl_2$: C, 40.8; H, 3.7; N, 8.2. Found: C, 41.0; H, 3.8; N, 8.3. EI-MS: *m/z* 474.

***cis,trans*-MoO(OSiMe$_3$)L.** A solution of $NaOSiMe_3$ (0.13g, 1.1 mmol) in THF (7 cm^3) was added dropwise to a stirred solution of *cis,cis*-[MoOClL] (0.25 g, 0.57 mmol) in THF (25 cm^3). After 1 h, the solvent was removed under vacuum, the residue extracted with CH_2Cl_2 (5 cm^3), and the extract applied to a silica gel 60 column (mesh 70−230, 40 cm × 1.4 cm diameter) in air. Upon elution with CH_2Cl_2 (elution rate 16 cm^3 min^{-1}), the first (red) band was collected, concentrated (4 cm^3), and layered with hexane (4 cm^3). Evaporation over 1 day yielded X-ray-quality crystals, which were washed with hexane and dried under vacuum (0.02 g, 7%). Anal. Calcd for $C_{19}H_{27}MoN_2O_2S_2Si$: C, 45.3; H, 5.4; N, 5.6. Found: C, 45.4; H, 5.3; N, 5.5. EI-MS: *m/z* 505. An alternative synthesis using *cis,trans*-[Mo^{VI}O$_2$L] and $(Me_3Si)_2S$ provides the same compound.[17]

***cis,trans*-MoO(OPh)L.** A solution of NaOPh (0.071 g, 0.61 mmol) in THF (7 cm^3) was added dropwise to a stirred solution of *cis,cis*-MoOClL (0.17 g, 0.37 mmol) in THF (20 cm^3). After 2 h, the solvent was removed under vacuum, the residue extracted with CH_2Cl_2 (7 cm^3), and the solution applied to a silica gel 60 column (mesh 70−230, 20 cm × 1.4 cm diameter) in air. Upon elution with CH_2Cl_2 (elution rate 11 cm^3 min^{-1}), the first (purple) band was collected. Evaporation of solvent yielded a purple microcrystalline solid (0.085 g, 45%). Anal. Calcd for $C_{22}H_{23}MoN_2O_2S_2$: C, 51.9; H, 4.6; N, 5.5; S, 12.7. Found: C, 52.1; H, 4.6; N, 5.5; S, 12.6. EI-MS: *m/z* 509. *cis,trans*-MoO(OPh)L (97 atom % ^{98}Mo; 45 atom % ^{17}OPh) was prepared similarly from *cis,cis*-[^{98}MoOClL] and NaOPh (45 atom % ^{17}O).

***cis,trans*-MoO(SPh)L.** A solution of NaSPh (0.11 g, 0.81 mmol) in EtOH (7 cm^3) was added dropwise to a stirred solution of *cis,cis*-[MoOClL] (0.16 g, 0.35 mmol) in thf (20 cm^3). After 2 h, the solvent was removed under vacuum, the residue extracted with CH_2Cl_2 (20 cm^3), and the solution applied to a silica gel 60 column (mesh 70−230, 15 cm × 2.3 cm diameter) in air. Upon elution with CH_2Cl_2 (elution rate 11 cm^3 min^{-1}), the first (green) band was collected. Evaporation of solvent yielded dark green microcrystals (0.045 g, 24%). Anal. Calcd for $C_{22}H_{23}MoN_2OS_3$: C, 50.5; H, 4.4; Cl, 0.0; N, 5.4; S, 18.4. Calcd for $C_{22}H_{23}MoN_2OS_3 \cdot {}^1/_4CH_2Cl_2$: C, 49.1; H, 4.4; Cl, 3.3; N, 5.1; S, 17.7. Found: C, 49.0; H, 4.3; Cl, 3.1; N, 5.1; S, 17.8. EI-MS: *m/z* 525.

***cis,trans*-MoOBrL.** This was isolated via chromatography from a crude sample of *cis,cis*-[MoOBrL]. A concentrated solution of *cis,cis*-[MoOBrL] (0.22 g, 0.45 mmol) in CH_2Cl_2 was applied to a silica gel 60 column (mesh 70−230, 40 cm × 2.3 cm diameter) in air. Upon elution with CH_2Cl_2 (elution rate 10 cm^3 min^{-1}), the first (green) band was collected, concentrated (3 cm^3), and layered with hexane (3 cm^3). Evaporation over 2 days yielded dark green crystals, which were washed with hexane and dried under vacuum (0.022 g, 0.045 mmol, 10%). Anal. Calcd for $C_{16}H_{18}BrMoN_2OS_2$: C, 38.9; H, 3.7; N, 5.7. Found: C, 38.9; H, 3.7; N, 5.6. EI-MS: *m/z* 495.

***C$_i$*-(MoOL)$_2$(*μ*-O).** A solution of $NaBPh_4$ (0.19 g, 0.56 mmol) in MeOH (13.5 cm^3) was added dropwise to a stirred solution of *cis,cis*-[MoOClL] (0.18 g, 0.40 mmol) in CH_2Cl_2 (15 cm^3). After 2.5 h, the solvent was removed under vacuum. The residue was extracted with CH_2Cl_2 (10 cm^3), the solution filtered through Celite, and thf (10 cm^3) added. The crude product was filtered off, washed with Et_2O, and dried under vacuum. X-ray-quality crystals were obtained by allowing an anaerobic, saturated solution in thf to stand at room temperature for 4 weeks. IR: ν(MoO) 942, ν(MoOMo) 424 cm^{-1}.

***C$_1$*-(MoOL)$_2$(*μ*-O).** Hexane (3 cm^3) was added to a solution of *cis,cis*-[MoO(OMe)L] (0.55 g, 0.12 mmol) in CH_2Cl_2 (6.5 cm^3). After 3 weeks, crystals that formed were removed, washed with hexane, and dried under vacuum (9.9 mg, 19%).

Physical Techniques. Powder infrared spectra were recorded on a Bio-Rad FTS-60A Fourier transform spectrometer using a Digilamp diffuse reflectance accessory in a KBr matrix. EPR spectra of fluid solutions (room temperature) or frozen glasses (77 K) were obtained on either a Bruker ECS 106 EPR spectrometer or Varian E-line spectrometer incorporating a Varian E-101 microwave bridge using diphenylpicrylhydrazyl (g = 2.0036) as a standard reference. UV−visible spectra were recorded on a Hitachi 150-20 spectrophotometer between 800 and 300 nm at a scan rate of 400 nm min^{-1}. Electron impact mass spectrometric measurements were made on a VG Micromass 7070F spectrometer operating at 70 eV. The EI-MS values quoted are those of the most intense peak in the parent ion isotope pattern. ^{1}H and ^{13}C NMR spectra were recorded on a Varian Unity 300 (300 MHz) or a Bruker Aspect 3000 (300 MHz) Fourier transform spectrometer using $CHCl_3$ (δ = 7.26) as an internal reference. Electrochemistry was performed using a Cypress CS-1090 electroanalysis system, Version 6.1/2V, and a Cypress CYSY-IR potentiostat. Solutions, typically 0.5 mM in 0.1 M supporting electrolyte, were anaerobically prepared and run under a stream of dinitrogen.

Voltammetry at macroelectrodes used glassy carbon (0.076 cm^2) and platinum (0.010 cm^2) diskworking electrodes. Voltammetry at microelectrodes used platinum (23 μm) and glassy carbon (12 μm) microelectrodes. The reference electrode consisted of a Ag/Ag$^+$ electrode incorporated into a double salt bridge containing supporting electrolyte to minimize contamination. The auxiliary electrode was a platinum wire. All systems were referenced to SCE using Fc/Fc$^+$ (0.39 V in MeCN, 0.57 V in CH_2Cl_2) as an internal standard.[18,19]

Crystal Structure Determinations. Single crystals of the mononuclear compounds were all grown by slow diffusion of a layer of hexane into a CH_2Cl_2 solution. Solutions of *cis,cis*-MoO(NCS)L were generated and maintained under anaerobic conditions. Isolation of single crystals of the binuclear compounds is described in the synthetic procedures given above.

Crystallographic data are given in Table 1 and positional parameters in the Supporting Information. Intensity data were collected on a Syntex P2$_1$ or an Enraf-Nonius CAD-4MachS single-crystal X-ray diffractometer using Mo Kα radiation (graphite crystal monochromator); λ = 0.710 73 Å. The data were corrected for Lorentz and polarization effects but not for extinction. Absorption corrections were applied for *cis,trans*-MoOClL, *cis,trans*-MoO(OSiMe$_3$)L, and *C*$_1$-(MoOL)$_2$(μ-O) only. All six structures were solved using a combination of Patterson map and difference synthesis and refined using a full-matrix least-squares procedure, with anisotropic temperature factors applied to each of the non-hydrogen atoms. The neutral-atom scattering factors used were taken from ref 20b, apart from those for the C, H, N, O, Si, and S atoms of the structures of *cis,trans*-MoOClL and *cis,trans*-MoO(OSiMe$_3$)L, which were those incorporated in the SHELX-76 program system.[21] Corrections were made for anomalous dispersion.[20c] Analyses of variance after the final refinements showed no unusual features. Further details for each of the structures are given below.

***cis,trans*-MoOClL.** Accurate cell parameters were obtained from least-squares refinement of the setting angles of 25 reflections in the range 22 < 2θ < 38°. Three reflections monitored after every 9600 s of X-ray exposure time showed no intensity variation. Absorption effects were numerically evaluated by Gaussian integration.[20a,21] The maximum and minimun transmission coefficients were 0.732 and 0.651. After anisotropic refinement of all atoms initially located (R = 0.16), the resulting difference map showed a peak of height 7.6 e Å^{-3} near the molybdenum atom, together with other peaks close to the sulfur, oxygen, and chlorine atoms, indicating that the structure was disordered. It was apparent that this disorder was due to some of the molecules in the crystal being rotated by approximately 180° about the pseudo-2-

(17) Wilson, G. L.; Kony, M.; Tiekink, E. R. T.; Pilbrow, J. R.; Spence, J. T.; Wedd, A. G. *J. Am. Chem. Soc.* **1988**, *110*, 6923.

(18) Bashkin, J. K.; Kinlen, P. J. *Inorg. Chem.* **1990**, *29*, 4507.

(19) Roberts, S. A.; Young, C. G.; Kipke, C. A.; Cleland, W. E., Jr.; Yamanouchi, K.; Carducci, M. D.; Enemark, J. H. *Inorg. Chem.* **1990**, *29*, 3650.

(20) Ibers, J. A., Hamilton, W. C., Eds. *International Tables for X-ray Crystallography*; The Kynoch Press: Birmingham, U.K., 1974: (a) Vol. IV, p 55; (b) Vol. IV, p 99; (c) Vol. IV, p 149. (Present distributor: Kluwer Academic Publishers, Dordrecht, The Netherlands.)

(21) Sheldrick, G. M. *SHELX-76: Program for Crystal Structure Determination*. University of Cambridge: Cambridge, U.K., 1976.

(22) *MoIEN: An Interactive Structure Solution Procedure*; Enraf-Nonius: Delft, The Netherlands, 1990.

Table 1. Crystallographic Data

	cis,trans-MoOOClL	*cis,cis*-MoOOClL	*cis,trans*-MoO(OSiMe$_3$)L	*cis,cis*-MoO(NCS)L	C_i-(MoOL)$_2$(μ-O)·thf	C_1-(MoOL)$_2$(μ-O)·CH_2Cl_2
formula	$C_{16}H_{18}ClMoN_2OS_2$	$C_{16}H_{18}ClMoN_2OS_2$	$C_{19}H_{27}MoN_2O_2SiS_2$	$C_{17}H_{18}MoN_3OS_3$	$C_{40}H_{52}Mo_2N_4O_5S_4$	$C_{33}H_{38}Cl_2Mo_2N_4O_3S_4$
color	dark blue-green	green-black	dark red	black	dark red	black
fw	449.9	449.9	503.6	472.5	989.0	929.7
size, mm	0. 48 × 0.40 × 0.34	0.25 × 0.35 × 0.75	0.05 × 0.48 × 0.48	0.08 × 0.08 × 0.73	0.66 × 0.22 × 0.15	0.30 × 0.33 × 0.45
a, Å	10.440(2)	13.564(4)	15.923(3)	22.471(2)	8.5650(5)	12.5250(5)
b, Å	14.260(2)	7.172(2)	11.141(2)	12.136(2)	15.1862(9)	24.673(1)
c, Å	12.041(2)	18.242(6)	14.186(2)	7.138(1)	16.8038(9)	12.7253(6)
β, deg	102.76(2)	95.19(1)	112.64(2)		100.183(1)	108.070(4)
V, Å^3	1748(1)	1767(2)	2323(1)	1947(1)	2157.1(8)	3738.6(3)
Z	4	4	4	4	2	4
space group	$P2_1/n$	$P2_1/c$	$P2_1/c$	$Pna2_1$	$P2_1/c$	$P2_1/c$
ρ, g cm^{-3}	1.71	1.69	1.44	1.61	1.52	1.65
μ, cm^{-1}	10.9	11.1	7.7	9.8	8.0	10.5
scan method	$\omega/2\theta$	$\omega/2\theta$	$\omega/2\theta$	$\omega/2\theta$	$\omega/2\theta$	$\omega/2\theta$
no. of data	5223	3551	6800	2017	4244	7069
no. of unique data	4011	3120	5326	1869	3793	6561
$2\theta_{max}$, deg	55	50	55	50	50	50
weights (*w*)	$7.066[\sigma^2(F) + 0.000007F^2]^{-1}$	$4F_o^2/\sigma^2(F_o^2)$	$1.840[\sigma^2(F) + 0.0003F^2]^{-1}$	$4F_o^2/\sigma^2(F_o^2)$	$4F_o^2/\sigma^2(F_o^2)$	$4F_o^2/\sigma^2(F_o^2)$
no. of data refined	3495 ($F_o^2 > 2\sigma(F_o^2)$)	2032 ($F_o^2 > 3\sigma(F_o^2)$)	3363 ($F_o^2 > 2\sigma(F_o^2)$)	1291 ($F_o^2 > 3\sigma(F_o^2)$)	2362 ($F_o^2 > 3\sigma(F_o^2)$)	4995 ($F_o^2 > 3\sigma(F_o^2)$)
R^a	0.052	0.038	0.037	0.032	0.046	0.043
R_w^b	0.061	0.052	0.044	0.041	0.078	0.056
shift/esd	0.00	0.00	0.00	0.02	0.09	0.06
max diff peak, e·Å^{-3}	0.58	0.73	0.38	0.35	1.2	1.3

^{a} $R = \sum||F_o| - |F_c||/\sum|F_o|$. ^{b} $R_w = \sum w||F_o| - |F_c||^2/\sum w|F_o|^2$.

fold axis. Both components were included in the refinement, with the assignment of a refinable site occupation factor. For the minor component, anisotropic temperature factors were able to be assigned only to the Mo, S, and O atoms, while the N and C atoms were assigned isotropic temperature factors. During the refinement, the carbon and nitrogen atoms of the minor component were constrained to ideal geometry, with the phenyl ring C−C distances being 1.395 Å, the phenyl C−N distances being 1.46 Å, the aliphatic C−N distances being 1.51 Å, and the C8−C9 distance being 1.50 Å. All hydrogen atoms were located for the major component and were fixed at geometrical estimates but not included in the refinement; no hydrogens were included for the minor component. Final refinement gave $R = 0.052$ and $R_w = 0.061$,with the maximum peak height being 0.58 e Å^{-3}, near the two positions of the molybdenum atom. The final occupancy factors for the two components were 0.722(5) and 0.278(5), respectively. Structure solution and refinement were carried out using the programs SHELXS-86 and SHELX-76.[21,23]

***cis,cis*-MoOOClL.** Accurate cell parameters were obtained from least-squares refinement of the setting angles of 34 reflections in the range $20 < 2\theta < 30°$. Three reflections monitored after every 97 reflections showed no intensity variation. All H atoms were placed in idealized positions and constrained using the riding model, the methyl group hydrogen positions being initially located from a difference map. The refinement converged with $R = 0.038$ and $R_w = 0.052$. Two residual electron density peaks in the final difference map are significant, being 0.730 and 0.654 e Å^{-3}, both approximately 1.1 Å from the Mo atom. An attempted absorption correction based on ψ-scan data resulted in no significant changes in positional or displacement parameters, but significantly worse refinement indices; the final *R* and R_w values increased to 0.043 and 0.057, respectively, while the heights of the residual electron density peaks also increased to 1.067 and 0.981 e Å^{-3}. The final structure is reported without absorption corrections applied to the data. All calculations were performed using MolEN software.[22]

***cis,trans*-MoO(OSiMe$_3$)L.** Accurate cell parameters were obtained from least-squares refinement of the setting angles of 25 reflections in the range $36 < 2\theta < 44°$. Three reflections were monitored after every 9600 s X-ray exposure time showed a 4% decrease in intensity; corrections were applied to the data. Absorption effects were numerically evaluated by Gaussian integration.[20a,21] The maximum and minimun transmission coefficients were 0.959 and 0.727. All of the hydrogen atoms, located from the difference map, were constrained at geometrical estimates with a common isotropic temperature factor being assigned to the hydrogens on each methyl carbon and each aromatic ring. Final refinement converged with $R = 0.037$ and $R_w = 0.044$, the maximum peaks in the final difference map being 0.38 e Å^{-3}, near the molybdenum atom. Structure solution and refinement were carried out using the programs SHELXS-86 and SHELX-76.[21,23]

***cis,cis*-MoO(NCS)L.** Accurate cell parameters were obtained from least-squares refinement of the setting angles of 31 reflections in the range $9 < 2\theta < 21°$. Three reflections monitored after every 97 reflections showed no intensity variation. All H atoms were placed in idealized positions and constrained using the riding model, the three methyl hydrogen atoms being located initially from a difference map. The refinement converged with $R = 0.032$ and $R_w = 0.041$. All calculations were performed using MolEN software.[22]

C_i-(MoOL)$_2$(μ-O)·thf. Accurate cell parameters were obtained from least-squares refinement of the setting angles of 62 reflections in the range $20 < 2\theta < 30°$. Three reflections monitored after every 97 reflections showed no intensity variation. All H atoms were placed in idealized positions and constrained using the riding model. A difference map at this stage of refinement ($R = 0.07$ and $R_w = 0.13$) clearly indicated a five-membered ring, assumed to be a molecule of thf incorporated into the crystal. Subsequent refinements indicated that the thf molecule was disordered and not fully occupied. The thf was modeled as five half-occupied carbon atoms, since it was not possible to identify the oxygen atom position(s); the final refinement converged with $R = 0.048$ and $R_w = 0.078$. Using additional residual peaks found in the difference map, it was possible to refine 10 half-occupied carbon atoms to refinement indices of $R = 0.03$ and $R_w = 0.05$. However, the resulting distances and angles could not be interpreted into chemically reasonable solvent molecules, and so the additional atoms were not included in the final model. Atoms C21−C25 represent the thf molecule. Calculations were carried out with MolEN software.[22]

C_1-(MoOL)$_2$(μ-O)·CH_2Cl_2. Accurate cell parameters were obtained from least-squares refinement of the setting angles of 25 reflections in the range $20 < 2\theta < 30°$. Two reflections monitored every 60 min showed no intensity variation. An empirical absorption correction based

(23) Sheldrick, G. M. SHELXS-86: Program for Crystal Structure Solution. *Acta Crystallogr.* **1990**, *A46*, 467.

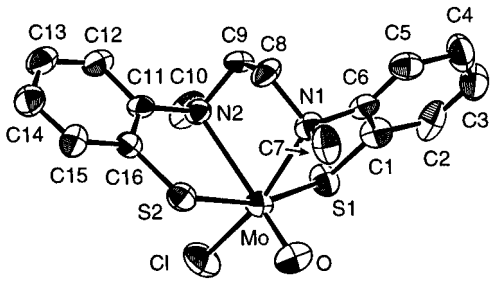

Figure 2. Molecular structure of *cis,trans*-MoOClL with 50% probability displacement. Hydrogen atoms are omitted.

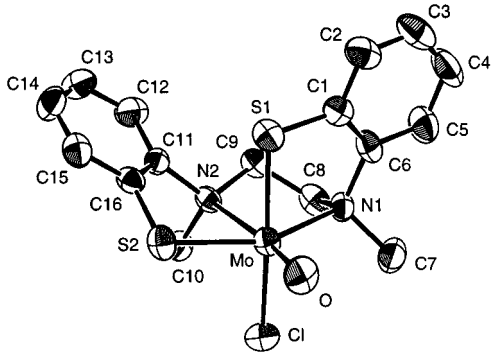

Figure 3. Molecular structure of *cis,cis*-MoOClL with 50% probability displacement. Hydrogen atoms are omitted.

on a series of ψ-scans was applied to the data. Relative transmission coefficients ranged from 0.764 to 0.999 with an average value of 0.875. All H atoms were placed in idealized positions and constrained using the riding model. The atoms of the methylene chloride solvent molecule (C51, Cl50, Cl52) were refined anisotropically. Initial attempts to refine the multiplicity of the solvent molecule and to refine the solvent as an isopropanol molecule were unsuccessful. The refinement converged with $R = 0.043$ and $R_w = 0.056$. Calculations were carried out with MolEN software.[22]

Results

Synthesis. The *cis,cis* isomer of MoOClL is isolated in 80% yield when LH_2 and $[MoOCl_5]^{2-}$ react in CH_2Cl_2/MeOH.[9] The product is freed from any contaminating *cis,trans* isomer by fractional crystallization. This material had been assumed previously to be the *trans,cis* form, but the crystal structure reported here (Figure 3) reveals its true nature. It can be converted to the thermodynamically more stable *cis,trans* form (Figure 2) by reflux in MeCN for 2 h. A similar approach using $[MoOBr_4]^-$ yields the two bromo analogs which could not be separated by fractional crystallization. Crystals of the *cis,cis* isomer can be separated manually. Chromatography of crude MoOBrL results in pure *cis,trans*-MoOBrL. *cis,cis*-MoOXL (X = OMe, OEt, NCS) and *cis,trans*-MoOXL (X = $OSiMe_3$, OPh, SPh) complexes were prepared by metathesis:

$$cis,cis\text{-MoOClL} + \text{NaX} \rightarrow \text{MoOXL} + \text{NaCl} \qquad (4)$$

Thermal rearrangement of *cis,cis*-MoO(NCS)L to the *cis,trans* form occurs readily in MeCN. EPR spectroscopy suggests that an equivalent rearrangement occurs when X = OMe, but attempted isolation via chromatography results in decomposition of the product. The siloxo derivative was prepared previously via a redox reaction between *cis,trans*-MoO_2L and $(Me_3Si)_2S$.[17]

Synthesis of [MoOL][BPh_4] was attempted via reaction 4 with X = BPh_4. However, the binuclear species C_i-$(MoOL)_2(\mu$-O)·thf was isolated in low yield. This product was also generated by refluxing *cis,cis*-MoO(OEt)L with H_2O in thf or by a redox reaction:

$$2cis,cis\text{-Mo}^{V}\text{O(OEt)L} + H_2O \rightarrow C_i\text{-(MoOL)}_2(\mu\text{-O}) + 2\text{EtOH} \qquad (5)$$

$$2cis,trans\text{-Mo}^{VI}\text{O}_2\text{L} + PPh_3 \rightarrow C_i\text{-(MoOL)}_2(\mu\text{-O}) + OPPh_3 \qquad (6)$$

Attempts to recrystallize *cis,cis*-MoO(OMe)L led to another binuclear isomer, C_1-$(MoOL)_2(\mu$-O)·CH_2Cl_2.

Electron impact mass spectrometry of each mononuclear complex yielded a molecular ion (see Experimental Section) having the expected isotope patterns. In particular, within experimental error, the mass spectra of each pair of *cis,cis*- and *cis,trans*-MoOXL (X = Cl, Br, NCS) isomers were identical (Figure S1, Supporting Information). Fragment ions centered at *m/z* 416, 401, 386, and 372 were evident in each spectrum, consistent with sequential loss of X, CH_3 (×2), and CH_2. Parent ions were not detected for the two binuclear species. In each case, the ion of highest *m/z* value was $[MoO_2L]^+$, consistent with cleavage of a Mo−O−Mo link.

Molecular Structures of MoOXL Complexes. Each molecule is six-coordinate with *cis* oxo and X ligands. The structural parameters of *cis,trans*-MoOClL (Figure 2, Table 2) are similar to those of characterized pseudooctahedral $[Mo^{V}OXN_2S_2]$ centers,[17,24,25] and the molecule is isostructural with *cis,trans*-$Mo^{VI}O_2L$. Metal−ligand bond lengths for *cis,trans*-MoOClL are unexceptional, but as expected, the distance Mo−N2 *trans* to the multiply-bonded oxo ligand is longer by 0.28 Å than Mo−N1 *trans* to chloro. This feature induces a larger bond angle for S1MoN1 than for S2MoN2 (81.8 versus 76.0°). The metal atom is displaced 0.35 Å toward the oxo ligand from the ClS1N1S2 plane while the phenyl rings define a dihedral angle of 92.6°.

Differential nonbonding repulsions between the oxo ligand and the two N(Me)C_6H_4S chelate pairs afford distinctly different OMoS bond angles of 106.2 and 90.1°. The larger angle OMoSl occurs when the MoO vector is perpendicular to the chelate plane, while the two are parallel for the smaller OMoS2 angle. The corresponding distances O···S are 3.26 and 2.91 Å, respectively, the latter being significantly shorter than the sum of the van der Waals radii (3.25 Å). Similar but less pronounced differences are seen as consequences of Cl···S interactions.

The molecule possesses three chiral centers, the Mo and two N atoms. The crystal is centrosymmetric and constructed from a racemic mixture of D-MoOCl(*R,R*-L) (Figure 2) and L-MoOCl(*S,S*-L) molecules.

cis,cis-MoOClL features *cis* thiolato sulfur atoms. Coordination spheres in the two isomers are compared in Figure 4a,b: N1 and S1 interchange positions. The differences are imposed by a difference in chirality at one nitrogen site. *cis,cis*-D-MoOCl(*S,R*-L) is shown in Figure 3; the racemic crystal contains L-MoOCl(*R,S*-L) as well. Compared to those in *cis,trans*-MoOClL (Table 2), the Mo−O and Mo−Cl distances are longer (0.03(1) and 0.06(1) Å, respectively) and the Mo−S distances shorter (0.02(1)−0.03(1) Å). The differential Mo−N distances remain, although N1 is now *trans* to S2 rather than C1. The presence of *cis* S atoms affects the detailed stereochemistry in a number of ways. The displacement of the metal toward the oxo ligand becomes more pronounced (0.35 to 0.43 Å). The dihedral angle between phenyl rings increases from 92.6 to 112.1°.

While the relative orientations of the MoO vector and the chelate rings are unchanged, the OMoS angles are now similar

(24) Yamanouchi, K.; Enemark, J. H. *Inorg. Chem.* **1979**, *18*, 1626.
(25) Bruce, A.; Corbin, J. L.; Dahlstrom, P. L.; Hyde, J. R.; Minelli, M.; Steifel, E. I.; Spence, J. T.; Zubieta, J. *Inorg. Chem.* **1982**, *21*, 917.

Table 2. Selected Interatomic Distances (Å) and Angles (deg) for *cis,trans*- and *cis,cis*-MoOClL[a]

	cis,trans-MoOClL	*cis,cis*-MoOClL
MoO	1.640(6)	1.668(4)
MoCl	2.341(3)	2.403(2)
MoN1	2.243(7)	2.257(5)
MoN2	2.515(8)	2.478(5)
MoS1	2.398(6)	2.365(2)
MoS2	2.405(7)	2.381(2)
OMoCl	103.4(3)	94.0(2)
OMoN1	94.9(3)	107.6(2)
OMoN2	163.6(3)	174.4(2)
OMoS1	106.2(3)	100.7(2)
OMoS2	90.1(3)	100.6(2)
N1MoN2	76.9(3)	77.0(2)
N1MoS1	81.8(3)	81.2(1)
N1MoS2	90.8(3)	150.9(1)
S1MoS2	162.5(3)	86.72(6)
S2MoN2	76.0(3)	75.3(1)
ClMoN1	160.4(3)	89.4(1)
ClMoN2	87.0(3)	82.6(1)
ClMoS1	86.2(2)	164.34(7)
ClMoS2	96.2(3)	95.80(6)
O···C7	2.975(10)	3.416(9)
O···C10	4.999(10)	4.953(7)
O···S1	3.262(9)	3.137(5)
O···S2	2.914(9)	3.149(5)
O···Cl	3.154(7)	3.020(5)
Cl···C7	5.407(8)	3.318(7)
Cl···C10	3.336(9)	3.067(6)
S1···S2	4.747(9)	3.258(2)

[a] The numbers in parentheses are the estimated standard deviations for the last digits.

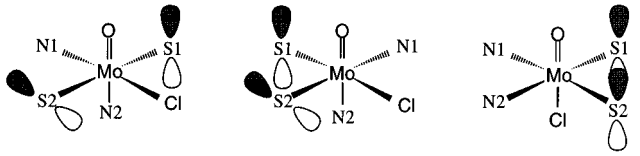

Figure 4. Coordination spheres for isomers of MoOClL, including relative orientations of sulfur p_π valence orbitals.

(100.7 and 100.6° versus 106.2 and 90.1°) and so are the O···S distances (3.14 and 3.15 Å versus 3.26 and 2.91 Å; cf. the sum of van der Waals radii, 3.25 Å). Both the OMoN1 (94.9 to 107.6°) and OMoN2 (163.6 to 174.4°) angles have opened. These features imply a lateral translation of the ligand backbone away from the oxo ligand with O and N1 consequently no longer in van der Waals contact.

In *cis,trans*-MoOClL, the *N*-Me substituents protrude on opposite sides of the molecule (Figure 2). In the *cis,cis* molecule, the change of configuration at one N atom means that both Me groups are on the same side of the ON1N2S2 plane (Figure 3). Both abut the Cl ligand (Cl···C10 = 3.07 Å; Cl···C7 = 3.32 Å), and C7 approaches the oxo ligand (O···C7 = 3.42 Å). The most acute angle around the oxo ligand is OMoCl which, at 94.0°, is much less than the 103.4° seen in the *cis,trans* isomer.

cis,trans-MoO(OSiMe$_3$)L (Figure 5, Table 3) is isostructural with *cis,trans*-MoO(OSiMe$_3$)L* (L*H$_2$ = *N,N*′-dimethyl-*N,N*′-bis(2-mercaptoethyl)ethylenediamine).[17] Minor structural changes compared to the case of *cis,trans*-MoOClL occur to accommodate the OSiMe$_3$ ligand in a structurally unhindered environment. The molybdenum−siloxo bond distance of 1.90 Å is similar to that seen in other molybdenum alkoxo complexes.[17,26,27] Comparison with *cis,trans*-MoOClL indicates the presence of differential nonbonded interactions between the terminal oxo and siloxo ligands and the chelate rings in *cis,trans*-

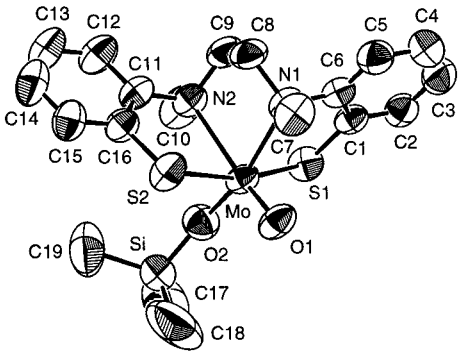

Figure 5. Molecular structure of *cis,trans*-MoO(OSiMe$_3$)L with 50% probability displacement. Hydrogen atoms are omitted.

Table 3. Selected Interatomic Distances (Å) and Angles (deg) for *cis,trans*-[MoO(OSiMe$_3$)L][a]

MoO1	1.668(3)	O2MoN2	85.4(1)
MoO2	1.903(3)	O2MoS1	87.4(1)
MoN1	2.294(3)	O2MoS2	93.8(1)
MoN2	2.453(3)	O1···C7	2.956(5)
MoS1	2.388(1)	O1···C10	4.941(5)
MoS2	2.434(1)	O1···S1	3.187(3)
O1MoO2	108.8(1)	O1···S2	2.988(3)
O1MoN1	91.2(1)	O1···O2	2.906(4)
O1MoN2	163.0(1)	O2···C7	4.990(5)
O1MoS1	102.1(1)	O2···C10	3.045(5)
O1MoS2	91.6(1)	S1···S2	4.782(1)
N1MoN2	76.2(1)	Si···O1	3.966(3)
N1MoS1	81.7(1)	Si···S1	4.504(2)
N1MoS2	92.3(1)	Si···S2	3.868(2)
S1MoS2	165.1(1)	S1···C17	4.964(6)
S2MoN2	77.8(1)	S2···C19	3.865(6)
O2MoN1	158.9(1)		

[a] The numbers in parentheses are the estimated standard deviations for the last digits.

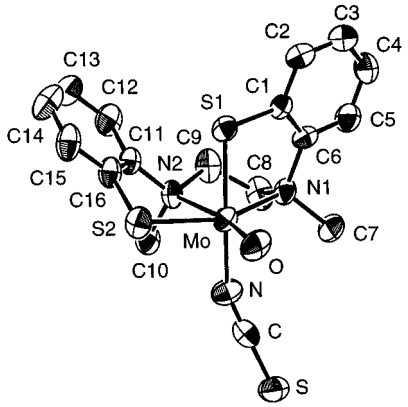

Figure 6. Molecular structure of *cis,cis*-MoO(NCS)L with 50% probability displacement. Hydrogen atoms are omitted.

MoO(OSiMe$_3$)L. In particular, sets of distinct O1MoS bond angles (102.1 and 91.6°), O1···S distances (3.19 and 2.99 Å), O2MoS bond angles (87.4 and 93.8°), and O2···S distances (2.99 and 3.19 Å) are seen.

cis,cis-MoO(NCS)L (Figure 6, Table 4) is isostructural with *cis,cis*-MoOClL, differences being consistent with the decrease in effective van der Waals radius due to substitution of chloro by nitrogen in the coordination sphere. The Mo−NCS distance of 2.10 Å is normal.[26] Steric interactions involving ligand methyl groups and the NCS ligand are apparent. The N···C7,C10

(26) Orpen, A. G.; Brammer, L.; Allen, F. H.; Kemmard, O.; Watson, D. G.; Taylor, R. *J. Chem. Soc., Dalton Trans.* **1989**, S1.
(27) Xiao, Z.; Bruck, M. A.; Enemark, J. H.; Young, C. G.; Wedd, A. G. *J. Biol. Inorg. Chem.* **1996**, *1*, 415.

Table 4. Selected Interatomic Distances (Å) and Angles (deg) for *cis,cis*-[MoO(NCS)L][a]

MoO1	1.691(7)	S1MoS2	87.33(9)
MoN	2.101(9)	S2MoN2	75.3(2)
MoN1	2.265(8)	NMoN1	86.5(3)
MoN2	2.447(7)	NMoN2	81.5(3)
MoS1	2.356(2)	NMoS1	164.4(3)
MoS2	2.380(3)	NMoS2	98.1(2)
O1MoN	92.0(4)	O1···C7	3.47(1)
O1MoN1	110.4(3)	O1···C10	4.88(1)
O1MoN2	170.2(3)	O1···S1	3.166(7)
O1MoS1	101.7(3)	O1···S2	3.118(6)
O1MoS2	98.6(3)	O1···N	2.74(1)
N1MoN2	76.7(3)	N···C7	3.17(1)
N1MoS1	81.8(2)	N···C10	2.93(1)
N1MoS2	150.6(2)	S1···S2	3.270(3)

[a] The numbers in parentheses are the estimated standard deviations for the last digits.

Table 5. Infrared Maxima (cm^{-1}) of MoOXL and $(MoOL)_2(\mu$-O)

MoOXL				
X	isomer	ν(Mo═O)		intensity at 895 > 845 cm^{-1} [a]
Cl	*cis,cis*	946		yes
	cis,trans	962		no
Br	*cis,cis*[b]	945		yes
	cis,trans	962		no
NCS	*cis,cis*	941	2038 (NCS)	yes
	cis,trans	953	2033 (NCS)	no
OMe	*cis,cis*	941, 935	1057 (CO)	yes
			515 (Mo−O)	
OEt		945, 939	1056 (CO)	yes
			516 (Mo−O)	
$OSiMe_3$	*cis,trans*	956	910 (SiO)	no
			837 (SiC)	
OPh		934	1249 (CO)	no
			634 (Mo−O)	
SPh		928		no
C_i-$(MoOL)_2(\mu$-O)		950	423 (MoOMo)	
C_1-$(MoOL)_2(\mu$-O)		942	424 (MoOMo)	

[a] Criterion of stereochemistry (see text). [b] Sample is analytically pure but contains ca. 15% of *cis,trans* form.

distances of 3.17 and 2.93 Å are both less than the van der Waals contact of 3.25 Å.

Spectroscopic Characterization of MoOXL Complexes. Infrared data for powdered samples are listed in Table 5. Each molecule exhibits a strong absorption in the range 928−962 cm^{-1}, readily assignable to ν(Mo═O).[28] The assignments of ν(Mo−OPh) and ν(O−C) at 634 and 1249 cm^{-1}, respectively, for MoO(OPh)L were confirmed by ^{17}O substitution. *cis,cis*- and *cis,trans*-MoOClL show differences in the fingerprint range 400−1400 cm^{-1} (Figure S2, Supporting Information). Most apparent is the reversal of relative intensities of the features at about 845 and 895 cm^{-1}. This difference is conserved in the other structurally characterized examples, *cis,trans*-MoO(OSiMe$_3$)L and *cis,cis*-MoO(NCS)L, and is the basis for the stereochemical assignments given in Table 5. With the exception of *cis,trans*-MoO(OSiMe$_3$)L, the lack of other prominent peaks in the region makes this method of assignment routine.

Each MoOXL complex is stable in solution at room temperature for extended periods under anaerobic conditions. Electronic spectra (Table S1) are similar in the 300−800 nm region, exhibiting strong absorption bands near 400 and 600 nm consistent with S(p) to Mo(d) charge transfer bands of the type seen in $[MoO(SR)_4]^-$.[14] The qualitative appearance of the lower energy band provides another basis for stereochemical assignment. As seen in Figure 7, the *cis,cis* isomers show a prominent

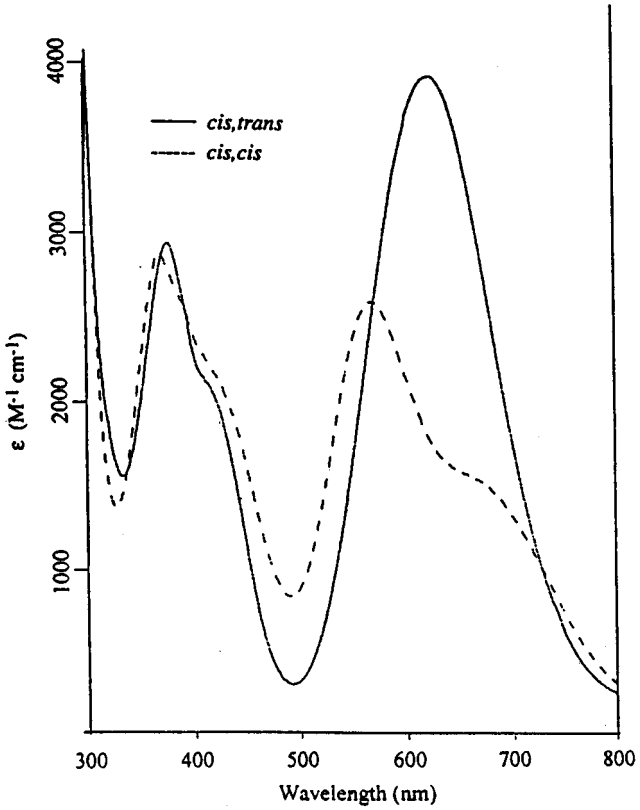

Figure 7. Electronic spectra of MoOClL in MeCN.

shoulder on the low-energy side of this band. Such assignments (Table S1, Supporting Information) are consistent with the available X-ray structural data and agree with those made by infrared spectroscopy (Table 5).

EPR spectra for mobile and frozen solutions are listed in Table S2, Supporting Information. The presence of an electrolyte such as $[Bu_4N][BF_4]$ was required for adequate resolution of frozen-solution spectra (Figure 8). The spectrum of each MoOBrL isomer in mobile solution exhibits well-resolved $^{79,81}Br$ ($I = {}^3/_2$) hyperfine coupling, similar in magnitude to that observed in $MoOBr(qtl)_2$ (7×10^{-4} cm^{-1}).[29] The observation is consistent with the presence of a *cis*-[MoOBr] fragment in each isomer.

The phenolic oxygen atom in *cis,trans*-MoO(OPh)L was enriched to 45 atom % ^{17}O ($I = {}^5/_2$) and the molybdenum atom to 97 atom % ^{98}Mo ($I = 0$). The EPR spectrum in thf at room temperature exhibited the six-line spectrum of $^{98}MoO(^{17}OPh)L$ overlapping the single resonance of $^{98}MoO(^{16}OPh)L$ (Figure 9). The separation of the two outer resonances allows estimation of $a(^{17}O)$, 4.9×10^{-4} cm^{-1}.

Electrochemistry. Cyclic voltammograms of *cis,trans*-MoO(OPh)L at a 3 mm diameter glassy carbon electrode in MeCN reveal an oxidation at 665 mV vs SCE and a reduction at −820 mV (Figure 10). Quantitative data are consistent with both processes being reversible, one-electron events (Table 6).[30] Steady state voltammograms at a platinum microelectrode (23 μm diameter) support this conclusion: plots of E versus $\ln(i_L - i)/i$ are linear, the slopes providing estimates of 1.0 for the number of electrons, n, transferred in the processes (X = OPh)[31−33]

$$[Mo^{VI}OXL]^+ + e^- = Mo^{V}OXL \quad (7)$$

$$Mo^{V}OXL + e^- = [Mo^{IV}OXL]^- \quad (8)$$

Each *cis,trans* compound studied featured a reversible or quasi-reversible couple, eq 8 (Table 7). An oxidative process

(28) Stiefel, E. I. *Prog. Inorg. Chem.* **1977**, *22*, 1.

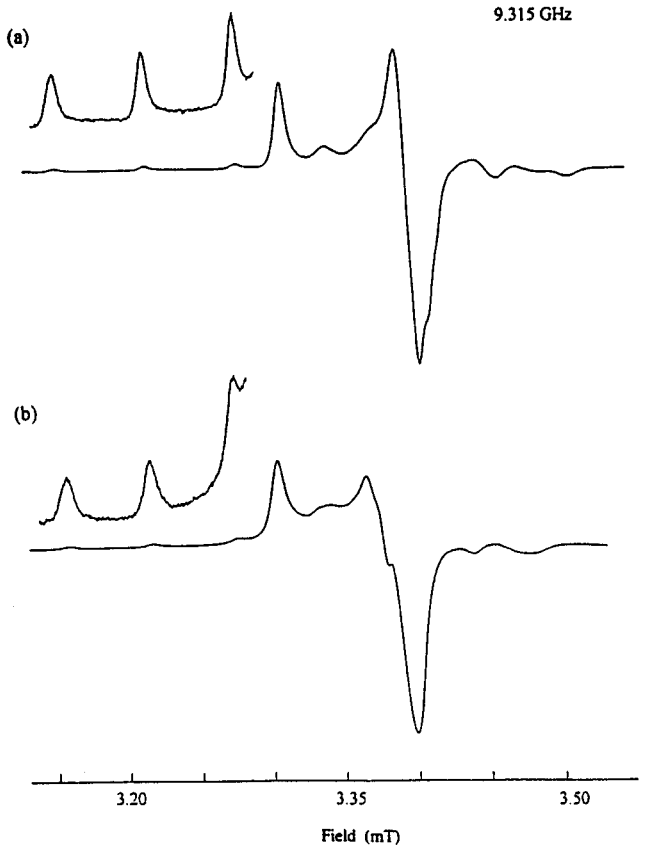

Figure 8. EPR spectra of MoOClL in a 10:1 thf:MeCN mixture, 0.1 M $[Bu_4N][BF_4]$, at $T = 77$ K: (a) *cis,cis*; (b) *cis,trans*.

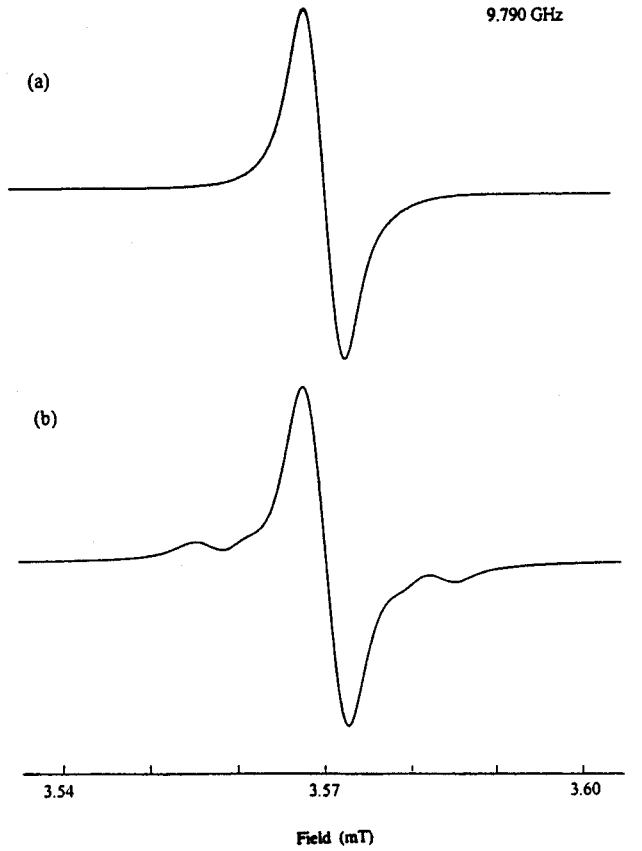

Figure 9. EPR spectra of *cis,trans*-MoO(OPh)L (^{98}Mo, 97 atom %) in thf at room temperature: (a) ^{16}OPh, 100 atom %; (b) ^{17}OPh, 45 atom %.

whose reversibility depended upon ligand X was also present. For example, *cis,trans*-$MoO(OSiMe_3)L$ features a clean reduction, eq 8 ($E_{1/2} = -1105$ mV), in MeCN when scanned cathodically but complex and irreversible oxidations in the range of 540−580 mV when scanned anodically. A reversible couple dependent upon the oxidation appears at −990 mV, identified as the couple *cis,trans*-$Mo^{VI}O_2L/[Mo^{V}O_2L]^-$.[9] Equations 9 are a plausible interpretation.

$$Mo^{V}O(OSiMe_3)L \rightarrow e^- + [Mo^{VI}O(OSiMe_3)L]^+ \quad (9a)$$

$$[Mo^{VI}O(OSiMe_3)L]^+ + H_2O \rightarrow Mo^{VI}O_2L + Me_3SiOH + H^+ \quad (9b)$$

The kinetically stable *cis,cis* isomers are characterized by generally irreversible electrochemical behavior (Table 7). While *cis,trans*-MoOClL exhibits a quasi-reversible reduction, eq 8, in MeCN containing the electrolyte Bu_4NBF_4 or Bu_4NCl, that for the *cis,cis* isomer is irreversible in Bu_4NBF_4. In the presence of excess Cl^-, the process approaches chemical reversibility: $i_{pa}/i_{pc} = 0.9$ at V, 200 mV s^{-1}. In each of the available *cis,cis*-MoOXL complexes (X = Cl, Br, OMe, $OSiMe_3$), reduction is coupled to an irreversible oxidation at about −20 mV, tentatively assigned to oxidation of $Mo^{IV}OL$ produced by dissociation of ligand X^- from $[Mo^{IV}OXL]^-$.

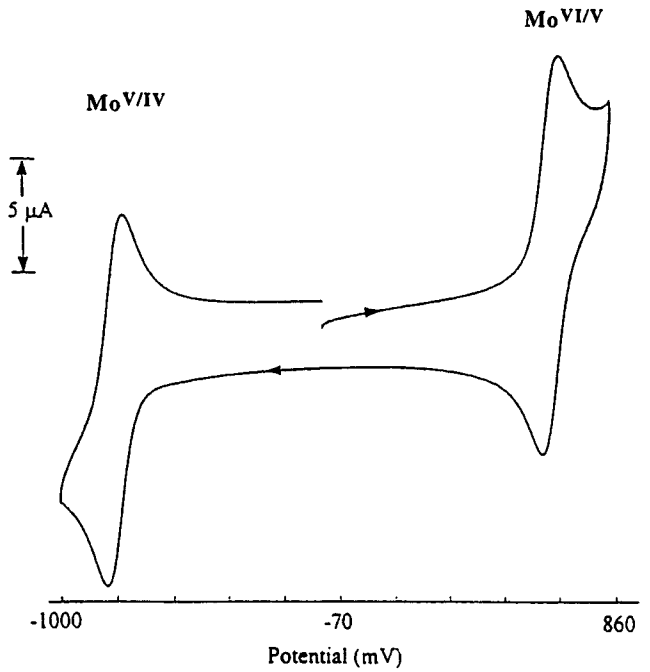

Figure 10. Cyclic voltammogram of *cis,trans*-MoO(OPh)L in MeCN (0.5 mM; 0.13 M $[Bu_4N][BF_4]$; 21 °C; 100 mV s^{-1}).

(29) Boyd, I. W.; Wedd, A. G. *Aust. J. Chem.* **1984**, *37*, 293.
(30) Bard, A. J., Faulkner, L. R., Eds. *Electrochemical Methods: Fundamentals and Applications* Wiley: New York, 1980; Chapter 4.
(31) Montenegro, M. I., Queirós, M. A., Daschbach, J. L., Eds. *Microelectrodes: Theory and Applications*; Kluwer Academic Publishers: Dordrecht, The Netherlands, 1991.
(32) Bond, A. M.; Oldham, K. B.; Zoski, C. G. *Anal. Chim. Acta* **1989**, *216*, 177.
(33) For the reduction, steady state voltammograms at $v = 10$ mV s^{-1} showed an oxidative return wave which did not closely retrace the reductive wave, suggesting irreversibility. This result is surprising, given the strong evidence for electrochemical reversibility at macroelectrodes (Table 8) and that the rate of diffusion of electroactive material to and from a microelectrode is intrinsically faster than that for a macroelectrode.[29] However, at higher scan rates (20−50 mV s^{-1}), the behavior was that expected for a reversible process. A likely explanation is interference due to adsorption of products to the electrode surface at the slow scan rate of 10 mV s^{-1} employed to ensure steady state conditions.

Table 6. Cyclic Voltammetric Data for *cis,trans*-MoO(OPh)L[a]

v, mV s^{-1}	E_{pa}, mV	E_{pc}, mV	ΔE_p, mV	$E_{1/2}$, mV	i_{pa}, mA M^{-1}	i_{pc}, mA M^{-1}	i_{pa}/i_{pc}	$i_{pc}v^{-1/2}$, mA $s^{1/2}$ $mV^{-1/2}$
				Couple 7				
20	685	626	59	656	6.6	6.4	1.1	45.4
50	684	624	60	654	10.1	10.0	1.0	44.7
100	684	623	61	654	13.8	13.7	1.0	43.3
200	688	617	71	653	18.2	18.4	1.0	41.1
500	691	620	71	656	30.4	30.0	1.0	42.4
1000	694	617	77	656	42.3	42.9	1.0	42.9
				Couple 8				
20	−789	−848	59	−819	6.6	6.4	1.0	45.0
50	−789	−851	62	−820	9.7	9.6	1.0	42.8
100	−787	−850	63	−819	14.2	13.7	1.0	43.2
200	−784	−854	70	−819	18.6	18.8	1.0	42.0
500	−783	−859	76	−821	30.4	29.6	1.0	41.9
1000	−778	−862	84	−822	44.4	45.7	1.0	45.7

[a] 0.52 mM; 0.10 M Bu_4NBF_4; MeCN; 19 °C; glassy carbon electrode (area 0.076 cm^2). Potentials versus SCE with ferrocene as an internal standard.

Table 7. Electrochemical Data for MoOXL in MeCN[a,b]

X	isomer	electrolyte anion[c]	reversibility	$E_{1/2}$[d] or E_p,[e] mV	ΔE_p,[e] mV	i_{pa}/i_{pc}	n[f]
OPh	*cis,trans*	BF_4^-	rev	655	61	1.0	1.0
			rev	−820	63	1.0	1.0
SPh[g]			irrev	945	88	1.7	
			q-rev	−460	86	1.1	1.0
$OSiMe_3$			irrev	560			
			rev	−1105	68	1.1	0.9
Cl			irrev	960			
			q-rev	−585	63	1.1	1.0
		Cl^-	q-rev	−570	63	1.0	1.0
	cis,cis	BF_4^-	irrev	1030			
			irrev	−470			
		Cl^-	q-rev	−500	71	0.8	1.0
Br	*cis,trans*	BF_4^-	q-rev	965	69	1.2	0.9
			q-rev	−540	72	0.8	1.1
	cis,cis		irrev	1000			
			irrev	−340			
NCS	*cis,trans*		q-rev	985	102	1.0	
			q-rev	−370	63	1.0	1.0
	cis,cis		irrev	990			
			irrev	−390			
OMe			irrev	460			
			q-rev[h]	−1020	73	1.0	1.0

[a] Potentials versus SCE with ferrocene as an internal standard. [b] 0.4−0.6 mM. [c] 0.10−0.16 M, Bu_4N^+ salt. [d] Estimated from cyclic voltammetry at a glassy carbon electrode (diameter 3 mm) or steady state voltammetry at a platinum microelectrode (diameter 23 μm). Quoted for rev or q-rev processes only. [e] Observed by cyclic voltammetry (v = 100 mV s^{-1}). E_p quoted for irrev processes. [f] Estimated from the slope of the graph E versus $\ln[(i_l - i)/i]$ derived from steady state voltammetry. [g] In CH_2Cl_2. [h] Parameters are those derived for v = 200 mV s^{-1}. At 100 mV s^{-1}, ΔE_p = 60 mV and i_{pa}/i_{pc} = 0.7.

Binuclear $(MoOL)_2(\mu$-O) Complexes. C_i-$(MoOL)_2(\mu$-O) exhibits an *anti* conformation for the terminal oxo ligands with equivalent pseudooctahedral molybdenum environments similar to those observed for *cis,trans*-MoOXL (X = Cl, $OSiMe_3$) (Figure 11, Table 8). The bridging Mo−O2 distance of 1.867 Å is similar to that in $Mo_2O_3L^*_2$, the only other binuclear Mo(V) complex with a tetradentate N_2S_2 ligand which has been characterized structurally.[34]

Three structural features require comment upon comparison with the *cis,trans* mononuclear structures (Tables 2, 3, and 8): (i) the Mo−S2 distance of 2.47 Å is longer than Mo−S1, 2.40 Å; (ii) angle XMoS1 has increased (91.8 (X = O2) versus 86.2 (Cl) and 87.4° ($OSiMe_3$)); (iii) angle XMoS2 has decreased (92.3 versus 96.2 and 93.8°). This feature of one normal and one longer Mo−S distance is also present in $Mo_2O_3L^*_2$. In both molecules, the longer distance is associated with the chelate ring MoN2CCS2 containing the ligand atom N2, *trans* to terminal oxo. It was presumed previously to reflect steric constraints imposed by the MoN1CCN2 chelate ring.[34] How-

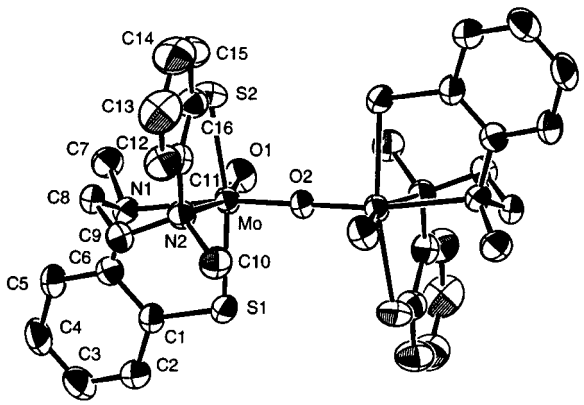

Figure 11. Molecular structure of C_i-$(MoOL)_2(\mu$-O)·thf with 50% probability displacement. Hydrogen atoms are omitted. Only atoms of the asymmetric unit are labeled: the unlabeled atoms are related centrosymmetrically through O2.

(34) Dahlstrom, P. L.; Hyde, J. R.; Vella, P. A.; Zubieta, J. *Inorg. Chem.* **1982**, *21*, 927.

Table 8. Selected Interatomic Distances (Å) and Angles (deg) for C_i-$(MoOL)_2(\mu$-O)·thf[a]

MoO1	1.685(5)	S1MoS2	163.15(8)
MoO2	1.867(6)	S2MoN2	76.7(1)
MoN1	2.320(6)	O2MoN1	162.4(2)
MoN2	2.470(6)	O2MoN2	87.4(1)
MoS1	2.398(2)	O2MoS1	91.75(5)
MoS2	2.469(2)	O2MoS2	92.29(6)
O1MoO2	106.0(2)	MoO2Mo	180
O1MoN1	91.5(2)	O1···C7	2.99(1)
O1MoN2	162.5(2)	O1···C10	4.944(9)
O1MoS1	103.4(2)	O1···S1	3.235(6)
O1MoS2	91.2(2)	O1···S2	3.018(6)
N1MoN2	76.0(2)	O1···O2	2.838(5)
N1MoS1	81.6(1)	O2···C7	4.979(8)
N1MoS2	89.7(2)	O2···C10	3.136(8)

[a] The numbers in parentheses are the estimated standard deviations for the last digits.

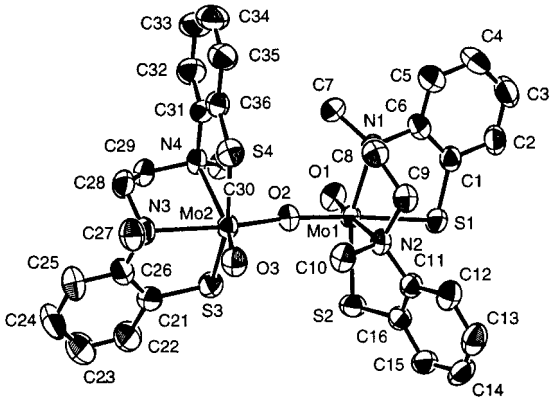

Figure 12. Molecular structure of C_1-$(MoOL)_2(\mu$-O)·CH_2Cl_2 with 50% probability displacement. Hydrogen atoms are omitted.

ever, *cis,trans*-MoOClL features equivalent Mo−S distances (Table 2: 2.40, 2,41 Å), as does *cis,trans*-MoO_2L.[9]

In contrast, different Mo−S distances are present in the following *cis,trans* compounds which feature bulkier X ligands: $MoO(OSiMe_3)L$ (Table 3: 2.39, 2.43 Å), $MoO(OSiMe_3)L$* (2.41, 2.46 Å),[17] and $Mo^{VI}O(N_2Ph_2)L$* (2.41, 2.48 Å).[35] In each of the mononuclear and binuclear systems, the longer Mo−S distance is associated with the five-membered chelate ring containing the N−Me ligand *trans* to the terminal oxo ligand. The methyl substituent projects toward X (O2 in this case: Figure 11), and the associated nonbonding interactions may play a role in the observed behavior. Apart from this possibility, no overt steric interaction between the equivalent halves of C_i-$(MoOL)_2(\mu$-O) is evident.

In C_1-$(MoOL)_2(\mu$-O), the terminal oxo ligands again assume an *anti* conformation but the two molybdenum environments are inequivalent, being *cis,cis* around Mo1 and *cis,trans* around Mo2 (Figure 12, Table 9). The effects of nonbonded interactions within and between the halves of the molecule are evident. On the *cis,trans* center (Mo2), bond distances and angles, including a long Mo2−S4 distance (2.47 Å), are comparable to those seen in C_i-$(MoOL)_2(\mu$-O) and are rationalized similarly. While bond lengths are within normal limits on the *cis,cis* center (Mo1), the terminal Mo1-O1 (1.69 Å) and bridging Mo1-O2 (1.93 Å) distances are longer and the angle O1Mo1O2 (99.3°) is smaller than those on the *cis,trans* side. In addition, the Mo1−S1 and Mo1−S2 distances are respectively 0.07 and 0.04 Å longer than those in *cis,cis*-MoOXL (X = Cl, NCS). As both *N*-Me substituents project into the bridged region of the molecule (Figure 12), the lengthening of both Mo−S distances is consistent with the argument that rationalized the presence of the single longer Mo−S2 distance in C_i-$(MoOL)_2(\mu$-O). Other features consistent with reduced steric interactions of the N−Me functions with O2 include a decrease in angles O1Mo1N1 (110.4 to 100.5°) and O2(N)Mo1S2 (98.1 to 91.4°) compared to *cis,cis*-MoO(NCS)L and a longer Mo1-O2 than Mo2-O2 distance (1.93 versus 1.86 Å).

Table 9. Selected Interatomic Distances (Å) and Angles (deg) for C_1-$(MoOL)_2(\mu$-O)]·CH_2Cl_2[a]

Mo1O1	1.686(4)	Mo2O3	1.674(4)
Mo1O2	1.926(3)	Mo2O2	1.857(3)
Mo1N1	2.240(4)	Mo2N3	2.326(4)
Mo1N2	2.461(4)	Mo2N4	2.479(4)
Mo1S1	2.431(1)	Mo2S3	2.388(2)
Mo1S2	2.423(1)	Mo2S4	2.472(2)
O1Mo1O2	99.3(2)	O3Mo2O2	107.1(2)
O1Mo1N1	100.5(2)	O3Mo2N3	90.1(2)
O1Mo1N2	176.0(2)	O3Mo2N4	159.8(2)
O1Mo1S1	96.6(1)	O3Mo2S3	103.4(2)
O1Mo1S2	106.7(1)	O3Mo2S4	89.5(1)
N1Mo1N2	76.6(2)	N3Mo2N4	75.6(2)
N1Mo1S1	81.5(1)	N3Mo2S3	80.8(1)
N1Mo1S2	151.1(1)	N3Mo2S4	91.1(1)
S1Mo1S2	85.73(5)	S3Mo2S4	164.64(6)
S2Mo1N2	75.8(1)	S4Mo2N4	76.8(1)
O2Mo1N1	93.9(1)	O2Mo2N3	161.8(2)
O2Mo1N2	83.7(1)	O2Mo2N4	89.0(1)
O2Mo1S1	164.0(1)	O2Mo2S3	89.3(1)
O2Mo1S2	91.4(1)	O2Mo2S4	94.9(1)
S1···S2	3.302(2)	Mo1O2Mo2	172.3(2)
O1···C7	3.225(7)	O3···C27	2.947(7)
O1···C10	4.994(7)	O3···C30	4.964(7)
O1···S1	3.114(1)	O3···S3	3.220(4)
O1···S2	3.327(4)	O3···S4	2.972(4)
O1···O2	2.757(5)	O3···O2	2.842(5)
O2···C7	3.204(6)	O2···C27	4.990(6)
O2···C10	2.959(7)	O2···C30	3.171(7)

[a] The numbers in parentheses are the estimated standard deviations for the last digits.

Bands assignable to ν(Mo═O) and symmetric ν(MoOMo) vibrations are apparent at 950 and 423 cm^{-1} in the C_1 complex and at 942 and 424 cm^{-1} in the C_i complex (Table 5). Unlike the case of the mononuclear complexes, comparison of the peak intensities at 895 and 845 cm^{-1} does not define the ligand stereochemistry unequivocally in these binuclear species. However, extra peaks and shoulders are apparent in the C_1 complex, indicative of the inequivalent *cis,cis* and *cis,trans* configurations about the two metal atoms.

While examination of the solution properties of the binuclear species was hampered by poor solubility, dissolution of C_i- or C_1-$(MoOL)_2(\mu$-O) produces indistinguishable electronic spectra (Table S1: λ_{max} (log ϵ) 394 (3.7), 562 (3.8), 750 (3.1)), consistent with a common equilibrium in solution. The spectra do not exhibit an absorption maximum in the 450−525 nm range, normally characteristic of $[(MoOL)_2(\mu$-O)$]^{4+}$ centers.[19,28,36] Each complex is EPR silent.

Discussion

The features which determine the structure of $[Mo^{VI}O_2]^{2+}$ ($4d^0$) complexes are well-understood.[28,37−40] The electronic influence of the strong π-donor oxo ligands dictates a *cis*

(35) Dahlstrom, P. L.; Dilworth, J. R.; Shulman, P.; Zubieta, J. *Inorg. Chem.* **1982**, *21*, 933.

(36) Craig, J. A.; Harlan, E. W.; Snyder, B. S.; Whitener, M. A.; Holm, R. H. *Inorg. Chem.* **1989**, *28*, 2082.

(37) Garner, C. D.; Bristow, S. In *Molybdenum Enzymes*; Spiro, T. G., Ed.; Wiley: New York, 1985; p 343.

(38) Stiefel, E. I. In *Comprehensive Coordination Chemistry*; Wilkinson, G., Gillard, R. D., McCleverty, J. A., Eds.; Pergamon Press: Oxford, U.K., 1987; Vol 3, p 1375.

stereochemistry. There is an accompanying *trans* influence leading to longer than normal bond distances for ligands *trans* to oxo. Anionic ligands normally bind *cis* to oxo, being stronger donors than neutral ligands. Ligand−ligand nonbonding interactions fine-tune the coordination spheres. Unusual stereochemistries can be traced to the influence of sterically demanding polydentate ligands.[41−45]

$[Mo^{V}O]^{3+}$ ($4d^1$) complexes tend to undergo condensation to spin-coupled, binuclear $[(Mo^{V}O)_2(\mu\text{-}O)]^{4+}$, $[(Mo^{V}O)_2(\mu\text{-}O)_2]^{2+}$, or related species.[28,38] Only three mononuclear complexes featuring bidentate or quadridentate N_2E_2 ligands (E = O, S) have been characterized structurally. Two of these, MoO(OSiMe$_3$)L* and MoOCl(qtl)$_2$ (qtlH = 8-mercaptoquinoline), are closely related to their $[Mo^{VI}O_2]^{2+}$ analogs, with an anionic ligand in the site previously occupied by the second oxo ligand.[17,24,46] The Mo═O, Mo−S, and Mo−N$_{trans}$ bond lengths in these two complexes are comparable to those of their $[Mo^{VI}O_2]^{2+}$ analogs. In the third case, [MoO(salen)(MeOH)]Br (salenH$_2$ = *N*,*N*′-ethylenebis(salicylideneamine)), steric constraints imposed by the quadridentate salen ligand force it to occupy the equatorial positions about the metal center, leaving a solvent molecule *trans* to the oxo group.[47]

Apart from the gross structural trends discussed above, some chelating ligands impose more subtle stereochemical effects upon the coordination spheres of $[Mo^{VI}O_2N_2E_2]$ and $[Mo^{V}OXN_2E_2]$ complexes. The influence of nonbonded interactions was first highlighted in the isomorphous pair $Mo^{VI}O_2(qtl)_2$ and $Mo^{V}OCl(qtl)_2$[24,46] and are particularly pronounced in species containing five-membered chelate rings. The structural parameters of *cis*,*trans*-MoOClL and *cis*,*trans*-MoO(OSiMe$_3$)L (Figures 2 and 5) are closely related to those of *cis*,*trans*-$Mo^{VI}O_2L$.[9] In each system containing ligand L or qtl, differential nonbonding interactions between the oxo ligand(s) and the chelate rings (oriented approximately parallel or perpendicular to the MoO vector) afford distinctly different OMoS angles and O···S distances (106.2 and 90.1° and 3.26 and 2.91 Å, respectively, in *cis*,*trans*-MoOClL). Similar but less pronounced differences are seen as a consequence of Cl···S interactions in the chloro compounds.

The *cis*-thiolato coordination in *cis*,*cis*-MoOXL (X = Cl, NCS; Figures 3 and 6) is novel, and the *cis* sulfur atoms are reminiscent of the ene-1,2-dithiolato binding in molybdenum enzymes.[7,8] However, the relative orientation of the two S p orbitals (Figure 4b) is different from that of an ene-1,2-dithiolate or a possible *trans*,*cis* isomer in the present system (Figure 4c). A *cis*-thiolato stereochemistry was observed previously in the complex $MoO_2(SCMe_2CH_2NHMe)_2$, whose distorted coordination sphere was described as a skew-trapezoidal bipyramid.[49,50] A combination of electronic and steric effects appears to determine the stereochemistry: a significantly covalent S···S interaction is implied by a S···S distance of only 2.8 Å:

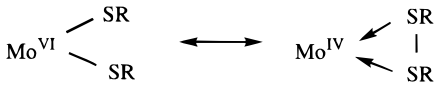

The S···S interatomic distance of 3.26 Å in *cis*,*cis*-MoOClL precludes any pronounced sulfur−sulfur covalent interaction and is similar to the S···S distance of 3.4 Å in {HB(Me$_2$pz)$_3$}MoO(SPh)$_2$, a six-coordinate complex in which the two thiolates are constrained to *cis* stererochemistry by the tris(pyrazolyl)borate ligand.[51] Isolation of the *cis*,*trans* isomer indicates that steric effects are not an overriding issue. However, it appears that a rearrangement from *cis*,*cis* to *cis*,*trans* isomers is favored by a more sterically demanding ligand X. *cis*,*cis*-MoOXL (X = Cl, Br, NCS) complexes, prepared at ambient temperature, convert to the *cis*,*trans* isomers upon heating in MeCN solution at 80 °C. Only the *cis*,*trans* form is isolated for systems with X = OSiMe$_3$, OPh, and SPh.

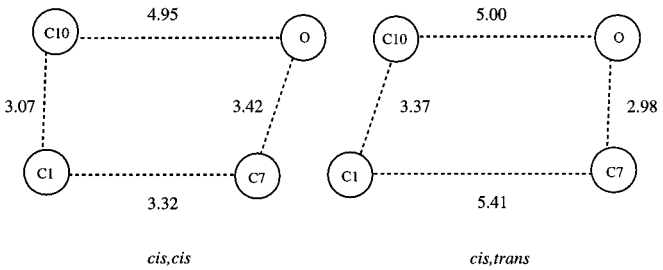

Figure 13. Selected interatomic distances (Å) in MoOClL isomers.

The relative orientations of the MoO vector and the chelate rings are the same in *cis*,*trans*- and *cis*,*cis*-MoOClL (Figure 4a,b). However, the two pairs of OMoS angles and O···S distances are similar in the *cis*,*cis* form (100.7, 100.6°; 3.14, 3.15 Å), contrasting with the marked differences discussed above for the *cis*,*trans* form (106.2, 90.1°; 3.26, 2.91 Å). These differences arise from a close contact between a methyl group and the chloro ligand in the *cis*,*cis* isomer (Figure 13). Van der Waals contact distances are estimated to be C···Cl = 3.35−3.60 Å and C···O = 3.15−3.20 Å.[52] The C10···Cl distance of 3.07 Å in the *cis*,*cis* form is very short and leads to the acute OMoCl angle (94.0 versus 103.4° in *cis*,*trans*). The MoO, MoS, and MoCl bond distances are similar in each isomer. Rearrangement to the *cis*,*trans* isomer relieves the very short C10···Cl contact distance, leading to a larger OMoCl angle and shorter MoO and MoCl bond distances. It also imposes a short C7···O contact of 2.98 Å, but overall, a more stable structure is attained.

The mechanism of rearrangement could not be studied because thermal conversion of the available *cis*,*cis* isomers led to significant yields of unknown products in addition to the *cis*,*trans* forms. The chirality at one of the nitrogen atoms is reversed in the rearrangement, indicating that dissociation of at least one ligand atom must occur, followed by an intramolecular rearrangement. As with other systems that result in exchange

(39) Hinshaw, C. J.; Peng, G.; Singh, R.; Spence, J. T.; Enemark, J. H.; Bruck, M.; Kristofzski, J.; Merbs, S. L.; Ortega, R. B.; Wexler, P. A. *Inorg. Chem.* **1989**, *28*, 4483.
(40) Nugent, W. A.; Mayer, J. M. *Metal-Ligand Multiple Bonds*; John Wiley & Sons, Inc.: New York, 1988.
(41) Hobday, M. D.; Smith, T. D. *Coord. Chem. Rev.* **1972**, *9*, 311.
(42) Villa, A. C.; Coghi, L.; Manfredotti, A. G.; Guastini, C. *Cryst. Struct. Commun.* **1974**, *3*, 551.
(43) Gullotti, M.; Pasini, A.; Zanderighi, G. M.; Ciani, G.; Sironi, A. *J. Chem. Soc., Dalton Trans.* **1981**, 902.
(44) Piggott, B.; Thorpe, S. D.; Sheppard; R. N. *Inorg. Chim. Acta* **1985**, *103*, L3.
(45) Berg, J. M.; Holm, R. H. *J. Am. Chem. Soc.* **1985**, *107*, 925.
(46) Yamanouchi, K.; Enemark, J. H. In *Proceedings of the Third International Conference on the Chemistry and Uses of Molybdenum*; Barry, H. F., Mitchell, P. C. H., Eds.; Climax Molybdenum Co.: Ann Arbor, MI, 1979; p 24.
(47) Gheller, S. F.; Bradbury, J. R.; Mackay, M. F.; Wedd, A. G. *Inorg. Chem.* **1981**, *20*, 3899.
(48) Kepert, D. L. *Prog. Inorg. Chem.* **1978**, *23*, 1.
(49) Stiefel, E. I.; Miller, K. F.; Bruce, A. E.; Corbin, J. L.; Berg, J. M.; Hodgson, K. O. *J. Am. Chem. Soc.* **1980**, *102*, 3624.
(50) Berg, J. M.; Spria, D. J.; Hodgson, K. O.; Bruce, A. E.; Miller, K. F.; Corbin, J. L.; Stiefel, E. I. *Inorg. Chem.* **1984**, *23*, 3412.
(51) Cleland, W. E., Jr.; Barnhart, K. M.; Yamanouchi, K.; Collison, D.; Mabbs, F. E.; Ortega, R. B.; Enemark, J. H. *Inorg. Chem.* **1987**, *26*, 1017
(52) Huhey, J. E.; Keiter, E. A.; Keiter, R. A. *Inorganic Chemistry*, 4th ed.; Harper Collins: New York, 1993; p 292.

of ligand atoms which are *cis* to the oxo ligand, the first step presumably involves dissociation of the atom N2 *trans* to the oxo ligand (Figure 4a,b).[53,54]

The steric bulk of ligand L alone is not sufficient to prevent binucleation. The complex C_i-$(MoOL)_2(\mu$-O) can be prepared conveniently in appreciable yield via reactions 5 or 6. A goal

$$\textit{cis,cis}\text{-MoO(OEt)L} + H_2O \rightarrow MoO(OH)L + EtOH \quad (5a)$$

$$MoO(OH)L + \textit{cis,cis}\text{-MoO(OEt)L} \rightarrow C_i\text{-}(MoOL)_2(\mu\text{-O}) + EtOH \quad (5b)$$

of the present work was to isolate $Mo^{V}O(OH)L$, previously stabilized in solution at low temperature.[9−11] This species is a plausible intermediate in reaction 5.

An equivalent pathway is possible in the reaction of *cis,cis*-MoOClL with $NaBPh_4$ to produce C_i-$(MoOL)_2(\mu$-O) and in the formation of the C_1 binuclear isomer from *cis,cis*-MoO(OMe)L. All attempts to isolate MoO(OH)L in substance have been unsuccessful. The $[Mo^{V}O(OH)]^{2+}$ center and its conjugate base $[Mo^{V}O_2]^{+}$ were obtained in systems based upon tridentate tris(pyrazolyl)borate ligands where an extra monodentate ligand is available for fine-tuning of steric and electronic properties.[55]

The structures of the two binuclear species, C_i-$(MoOL)_2(\mu$-O) (two *cis,trans* centers) and C_1-$(MoOL)_2(\mu$-O) (one *cis,trans*, one *cis,cis*), follow from those of the mononuclear complexes. Differences can be rationalized on the basis of *N*-methyl substituents interacting with the bridging region of the molecules (Figures 11 and 12).

C_1-$(MoOL)_2(\mu$-O) can be considered as a *cis,cis*-MoOXL derivative with X = $(\mu$-O)MoOL, a bulky substituent. This is an apparent contradiction of the previous conclusions that bulky X groups favor a *cis,trans* configuration. However, the presence of a relatively long Mo1O2 bond (1.93 versus Mo2O2, 1.86 Å) coupled with a nearly linear Mo1O2Mo2 moiety (172.3°; cf. MoNC angle in *cis,cis*-MoO(NCS)L) results in little steric clashing of the $(\mu$-O)MoOL fragment with the *N*-methyl substituents. In comparison, the MoOSi bond angle of 145.0° in *cis,trans*-$MoO(OSiMe_3)L$ is smaller. The resultant steric crowding is less acceptable in *cis,cis* complexes in which the *N*-methyl groups, particularly that of C10, are projected toward X (Figure 13). Consequently, although the bulk of X is important in the determination of ligand configuration in these species, its shape is crucial. In the two binuclear cases, a longer MoO2 distance and linear MoOMo fragment allow MoOXL (X = $(\mu$-O)MoOL) to be stable.

On the basis of four structurally characterized examples, infrared and electronic spectral criteria allow unambiguous identification of ligand stereochemistry in mononuclear MoOXL complexes (Figures 7 and S2; Tables 5 and S1). Spectroscopic and electrochemical properties of *cis,cis*-MoOClL clearly identify this as the complex reported earlier as *trans,cis*-MoOClL.[9] As part of that work, substitution reactions using this complex generated species in solution at ambient temperature which were believed to be MoOXL (X = OH, F). These were assigned as *trans,cis* on the basis of the assumed stereochemistry of the chloro precursor (now known to be the *cis,cis* complex) and the absence of coupling to ^1H or ^{19}F. The electronic spectra reported for these systems do not possess the shoulder characteristic of *cis,cis* complexes (cf. Figure 7), and so a simple substitution has not occurred. Consequently, the stereochemistry of the OH and F species is unknown.

The electronic spectra of the *cis,cis*- and *cis,trans*-MoOXL complexes are qualitatively strikingly similar (Figure 7, Table S1), and the large molar absorptivities imply that the bands have considerable sulfur to molybdenum charge transfer character. The effective site symmetry for each stereochemistry is C_1 (Figure 4a,b), and both structures give rise to the same two types of S(p)−Mo(d) bonding interactions. One interaction involves the S2 p orbital, which is constrained to be in the equatorial plane, and the Mo d_{xy} orbital (taking the MoO vector as the *z* direction). The other interaction involves the S1 p orbital, which is constrained to be out of the equatorial plane, and the d_{xz} (or d_{yz}) orbital. These interactions are distinctly different from those in *trans,cis* complexes or, equivalently, from those with chelating dithiolate ligands (see Figure 4c). Here, the S p orbitals interact primarily with the $d_{xz,yz}$ pair and are nearly orthogonal to d_{xy}. Magnetic circular dichroism studies of a variety of the latter complexes showed that splitting of the Mo d orbitals is dominated by the oxo ligand and varies little among such complexes.[56] The lowest energy transition in such species can be assigned to weak charge transfer transitions from the out-of-plane S p orbitals to the in-plane d_{xy} orbital. Similar detailed electronic studies are not available yet for the MoOXL species reported here and so assignment of their electronic spectra is not possible.

The electrochemical properties of MoOXL complexes depend upon both the stereochemistry of ligand L and the nature of ligand X (Table 7). *cis,cis* complexes exhibit irreversible redox behavior in general. The presence of excess Cl^- allows observation of a chemically reversible one-electron reduction in *cis,cis*-MoOClL (eq 8), apparently by suppressing dissociation of the chloro ligand in $[Mo^{IV}OClL]^-$. Each *cis,trans* compound features a chemically reversible one-electron reduction. The importance of ligand X is highlighted by the oxidative properties of the two *cis,trans* complexes with X = $OSiMe_3$ and OPh, each of which contains an O-bound ligand. Oxidation of MoO-$(OSiMe_3)L$ leads to elimination of the $OSiMe_3$ ligand and formation of $Mo^{VI}O_2L$ (eqs 9). On the other hand, MoO(OPh)L features a reversible one-electron oxidation (eq 7, Figure 12). Reversible access to molybdenum oxidation states VI, V, and IV is uncommon. It has been observed previously in Mo(V) tris(pyrazolyl)borate complexes (which feature OR ligands, as do the present species), in certain $[MoO(SR)_4]^-$ systems and in $Mo^{V}O$(mec) ($mecH_3$ = 2,3,17,18-tetramethyl-7,8,12,13-tetraethylcorrole).[25,57−60]

The isotropic solution EPR spectra of the MoOXL complexes show the large *g* and small $a(^{95,97}Mo)$ values commonly observed for oxo−Mo(V) centers with multiple thiolate ligands and low-lying S(p)−Mo(d_{xy}) charge transfer bands.[61−63] *cis,-trans*-MoO(SPh)L is a rare example of such a center with three thiolate ligands.[64] Its isotropic *g* and $a(^{95,97}Mo)$ values are intermediate to those for compounds with two and four thiolate

(53) Garner, C. D.; Hyde, M. R.; Mabbs, F. E.; Routledge, V. I. *J. Chem. Soc., Dalton Trans.* **1977**, 1198.
(54) Garner, C. D.; Hyde, M. R.; Mabbs, F. E.; Routledge, V. I. *J. Chem. Soc., Dalton Trans.* **1975**, 1175.
(55) Xiao, Z.; Gable, R.; Wedd, A. G.; Young, C. G. *J. Am. Chem. Soc.* **1996**, *118*, 2912.
(56) Carducci, M. D.; Brown, C.; Solomon, E. I.; Enemark, J. H. *J. Am. Chem. Soc.* **1994**, *116*, 11856.
(57) Soong, S.-L.; Chebolu, V.; Koch, S. A.; O'Sullivan, T.; Millar, M. *Inorg. Chem.* **1986**, *25*, 4067.
(58) Ueyama, H.; Zaima, H.; Nakamura, A. *Chem. Lett.* **1986**, 1099.
(59) Matsuda, Y.; Yamada, S.; Yukito, M. *Inorg. Chem.* **1981**, *20*, 2239.
(60) Chang, C. S. J.; Collison, J.; Mabbs, F. E.; Enemark, J. H. *Inorg. Chem.* **1990**, *29*, 2261.
(61) Garner, C. D.; Mabbs, F. E. *J. Inorg. Nucl. Chem.* **1979**, *41*, 1125.
(62) Deaton, J. C.; Solomon, E. I.; Watt, G. D.; Wetherbee, P. J.; Durfor, C. N. *Biochem. Biophys. Res. Commun.* **1987**, *149*, 424.
(63) Dhawan, I. K.; Enemark, J. H. Submitted for publication.
(64) Hahn, R.; Küsthardt, U.; Scherer, W. *Inorg. Chim. Acta* **1993**, *210*, 177.

groups.[14,63,65,66] The magnitude of $A_1(^{95,97}Mo)$ for *cis,trans*-MoO(SPh)L is typical of oxo−Mo(V) complexes.[67] Comparison of the anisotropic *g* components of *cis,trans*-MoO(SPh)L to those of the high-pH form of sulfite oxidase[65] shows that it exhibits a somewhat larger g_1 (2.023 versus 2.007) and a somewhat smaller g_3 (1.960 versus 1.968).

The phenolic oxygen atom in *cis,trans*-MoO(OPh)L (^{98}Mo, 97 atom %; $I = 0$) was enriched to 45 atom % ^{17}O ($I = {}^5/_2$), allowing estimation of $a(^{17}O)$ as 4.9×10^{-4} cm^{-1} (Figure 9). This value can be compared to those observed for *cis,trans*-[MoO(OH)L] (7.6×10^{-4} cm^{-1}) and -[MoO(OSiMe$_3$)L] (4.3×10^{-4} cm^{-1})[11,17] and in the Rapid Type 1 (6.3×10^{-4} cm^{-1}) and Rapid Type 2 (5.4×10^{-4} cm^{-1}) signals of XnO.[11,68] It appears that the magnitude of isotropic coupling to the OR oxygen in *cis*-MoO(OR) fragments is relatively insensitive to the nature of R.

(65) Dhawan, I. K.; Pacheco, A.; Enemark, J. H. *J. Am. Chem. Soc.* **1994**, *116*, 7911.
(66) Bradbury, J. R.; Mackay, M. F.; Wedd, A. G. *Aust. J. Chem.* **1978**, *31*, 2423.
(67) Carducci, M. D.; Enemark, J. H. To be published.
(68) Morpeth, F. F.; George, G. N.; Bray, R. C. *Biochem. J.* **1984**, *220*, 235.

Conclusions

The stereochemistry of ligand L observed in *cis*-MoOXL complexes depends upon the steric properties of anionic ligand X. A *cis-S,S* conformation leads to a short $H_3C\cdots X$ distance, which destabilizes that arrangement relative to the *trans-S,S* conformation. Infrared and electronic spectral data allow unambiguous identification of the stereochemistry of L in mononuclear complexes MoOXL.

Acknowledgment. K.R.B. acknowledges an Australian Postgradute Research Award, A.G.W. thanks the Australian Research Council for financial support (Grant No. 290 30599), and J.H.E. thanks the National Institutes of Health for financial support (Grant No. GM-37773).

Supporting Information Available: Tables S1−S24, listing atomic positional parameters, interatomic distances and angles, and anisotropic displacement parameters, Tables S25 and S26, listing electronic and EPR data, and Figures S1 and S2, showing mass and infrared spectra (29 pages). Ordering information is given on any current masthead page.

IC960848H